5-1-2014

Open quantum system dynamics for describing state transfer

Nayeli Zuniga-Hansen
Southern Illinois University Carbondale, nayelizh@gmail.com

A DISSERTATION ON OPEN QUANTUM SYSTEM DYNAMICS FOR DESCRIBING STATE TRANSFER

by

Nayeli Zuniga-Hansen

Ph.D., Southern Illinois University, 2013

A Dissertation
Submitted in Partial Fulfillment of the Requirements for the
Doctor of Philosophy Degree

Department of Physics
in the Graduate School
Southern Illinois University Carbondale
December, 2013

DISSERTATION APPROVAL

OPEN QUANTUM SYSTEM DYNAMICS FOR DESCRIBING STATE TRANSFER

By

Nayeli Zuniga-Hansen

A Dissertation Submitted in Partial

Fulfillment of the Requirements

for the Degree of

Doctor of Philosophy

in the field of Physics

Approved by:

Dr. Mark S. Byrd, Chair

Dr. Aldo Migone

Dr. Thushari Jayasekera

Dr. Eric Chitambar

Dr. Philip Feinsilver

Graduate School
Southern Illinois University Carbondale
June 24, 2013

AN ABSTRACT OF THE DISSERTATION OF

NAYELI ZUNIGA-HANSEN, for the Doctor of Philosophy degree in PHYSICS, presented on June 24, 2013, at Southern Illinois University Carbondale.

TITLE: OPEN QUANTUM SYSTEM DYNAMICS FOR DESCRIBING STATE TRANSFER

MAJOR PROFESSOR: Dr. Mark S. Byrd

In principle a quantum system could be used to simulate another quantum system. The purpose of such a simulation would be to obtain information about problems which are difficult to simulate on a classical computer due to the exponential increase of the Hilbert space with the size of the system, and which cannot be readily measured or controlled in an experiment. A quantum simulator is, however, an open quantum system that will interact with the surrounding environment, which in this case are other particles in the system, and will be implemented using imperfect controls, making it subject to noise. It has been suggested that noise does not need to be controlled to the same extent as it must be for general quantum information processing. However, the effects of noise in quantum simulations are not well understood and how best to treat them in most cases is not known. In the present work we study an existing quantum algorithm for the simulation of the one-dimensional Fano-Anderson model. This algorithm was proposed for a liquid-state NMR device. We examine models of noise in the evolution using different initial states in the original model. We also add interacting spins to simulate realistic situation where an environment of spins is present. We find that states which are entangled with their environment, and sometimes correlated but not necessarily entangled have an evolution which is described by maps which are not completely positive. We discuss the conditions for this to occur and also the implications.

ACKNOWLEDGMENTS

I would like to express my gratitude to my PhD advisor, Prof. Mark Byrd for his support and guidance.

I am also deeply grateful to Prof. Thushari Jayasekera, Prof. Eric Chitambar, Prof. Aldo Migone and Prof. Philip Feinsilver for agreeing to serve on my graduate committee.

Special thanks to Prof. Leonardo Silbert who, due to timing issues, could not serve on my graduate committee, but has been very supportive and helpful all through my PhD.

Also special thanks to Prof. Mercedes Calbi, for being my mentor before I began working with Prof. Byrd.

Thanks to my colleague Yu-Chieh Chi for collaborating with me in this project.

I also want to thank the SIUC physics department for their support and opportunities they provided for me.

And last, but not least I wish to thank my family for their support and encouragement.

TABLE OF CONTENTS

LIST OF FIGURES

CHAPTER 1

INTRODUCTION

1.1 INTRODUCTION

The rising interest in the field of open quantum system dynamics can be attributed to the possibility of building a quantum computer. Quantum information processing promises to perform tasks much more efficiently than classical computers, and they do so by relying on quantum superposition and entanglement. Quantum superposition implies that the state of a system can be in a linear combination of allowed states $|0\rangle$ and $|1\rangle$. However, this behavior is never observed in classical information processing.

According to Zurek [142, 143], the environment surrounding a quantum system imposes classical behavior by destroying coherences of preferred states, which he calls *pointer states* and are stable despite the environment, but the quantum superpositions of these states are not. The fragility of quantum correlations has proved a challenge in the quest to develop a quantum computing device. This, added to the fact that complete isolation of quantum mechanical systems is impossible, highlights the importance of understanding how noise affects quantum mechanical systems and how it can be controlled or minimized.

One of the central motivations to build a quantum computer was Feynman's idea of using a quantum system as a simulator to other quantum systems [141, 104, 83]. A quantum computer would perform as a universal quantum simulator, however, it is not necessary to have a fully functioning quantum computer to perform quantum simulations [74]. Recent experimental advances allow for the use of smaller, controllable quantum systems which are engineered to represent other quantum systems and mimic their dynamics. These are called quantum simulators. A device of this type not only requires less computational resources than a classical computer to simulate a relatively large Hilbert space, but behaves according to the laws of quantum mechanics, just like the systems it is

intended to represent. It is expected that quantum simulators may help provide answers to a variety of many-body problems for which no analytical solution is known, and for which numerical simulation requires more computational resources than those currently available. However, these are quantum systems, and are in contact with a reservoir which will induce noise in the system. And even though control has been achieved for relatively small systems, the problems of relevance are those that cannot be simulated in a classical computer (i.e. systems composed of more than 50 particles [74]). Scaling the size of the simulator has proved problematic since it is more challenging to control a larger number of particles. But there is also the problem of interactions of the particles with the environment and with other particles in the system. This can lead to unwanted correlations that can alter the physical quantity of interest.

Although it has been suggested that noise in quantum simulations does not need to be treated in the same was as for quantum computation, it is not known to what extent do errors affect the output of the simulation [109, 105]. Moreover, it is not known if the presence of initial correlations with either the environment or other particles in the system will also affect the final result. Quantum simulators are experimental devices which will be subject to many sources of noise and imperfections, studying the effects of these can help determine how they will affect the outcome and what useful information can be obtained.

Because a quantum simulator is a quantum system, one of the sources of noise and imperfections will be this interaction. And because the dynamics of a system in the presence of a noisy environment is described with dynamical maps, we also look at the effects that errors in the initialization of a quantum simulator have on the reduced dynamics.

Dynamical maps are expected to be completely positive, just like a unitary operator is, but this has been found to not always be the case. Some initial correlations may result in non completely positive dynamics, which can still describe the evolution of a quantum state, but the physical interpretation of non-complete positivity is not completely clear at

the moment. We look at different configurations of the initial state to find what class of states can yield a non completely positive dynamical map, and discuss the implications.

1.1.1 Arrangement of this dissertation

Most of the work presented in this dissertation has been published in [105], and has been organized in the next chapters.

Chapter 2 provides an introduction to open quantum system dynamics, starting from closed system evolution. The main subject is the definition of dynamical maps, which are used to describe the most general evolution of a quantum system. We review the characteristics of the map that make it adequate to describe quantum dynamics and recall that in the limit of closed quantum system dynamics, these maps become the unitary operator. Most research in this field is concerned with the concept of completely and not completely positive evolution, which are also defined.

Chapter 3 provides an introduction to quantum simulators. Quantum simulations in this context are experiments in which a quantum system is engineered to simulate another quantum system. The basic quantum simulation steps are: preparation of an initial state, time evolution and exctraction of quantities of interest. We review the different ways in which these tasks are performed and look into the classification of available and proposed quantum simulating devices.

In Chapter 4 the results of this research are summarized. Starting with the description of the quantum algorithm and the procedure followed to represent different types of errors. The outcome of the quantum simulation is analyzed when errors are present, and we also calculate the dynamical maps to describe the most general quantum evolution. Finally, in Chapter 5, we discuss our conclusions.

CHAPTER 2

OPEN QUANTUM SYSTEM DYNAMICS

2.1 CLOSED QUANTUM SYSTEM DYNAMICS

Classically, a closed system is one which does not exchange energy or particles with the environment [120, 13]. In quantum mechanics a closed, or isolated, quantum system is one which evolves *unitarily* according to the time dependent Schrödinger equation [61, 142, 13]

$$i\hbar\frac{d\left|\psi\right\rangle}{dt} = H\left|\psi\right\rangle \tag{2.1}$$

H is the Hamiltonian of the system, and $|\psi\rangle$ is a vector in the Hilbert space, $\mathcal{H}_{\mathcal{S}}$, of the system, and is a solution to the Schrödinger equation. The state vector $|\psi\rangle$ contains all the information about the state of the system. Is usually represented as a linear combination of the set of orthonormal basis states, $|\phi_i\rangle$, that span the space $\mathcal{H}_{\mathcal{S}}$:

$$\left|\psi\right\rangle = \sum_i \left|\phi_i\right\rangle\left\langle\phi_i\right|\left|\psi\right\rangle = \sum_i c_i\left|\phi_i\right\rangle \tag{2.2}$$

The complex coefficients, c_i, can be thought of as projections of the state $|\psi\rangle$ on each of the eigenvectors $|\phi_i\rangle$, and give the probability that the quantum system will be in the state $|\phi_i\rangle$ at a given time t, given by $\left|c_i(t)\right|^2$. And all the probabilities must satisfy $\sum_i \left|c_i(t)\right|^2 = 1$. Therefore Eq. (2.2) is in a *quantum superposition* of allowed states. The eigenvectors, $|\phi_i\rangle$, are usually solutions to the Schrödinger equation, and so is a linear combination of the form of Eq. (2.2).

In the classical world, objects are *localized*, their position and momentum can be measured precisely, but in the quantum world, a system can be in a superposition of states. Zurek [142, 143] defines the loss of quantum superpositions as the transition from quantum to classical, which occurs when the system is in contact with the environment. This

phenomenon is known as *decoherence*, *dephasing* or loss of quantum coherent superposition [142]. This point will be addressed again in this dissertation.

The solution to Eq. (2.1) is the propagator, or the unitary operator, U, that describes the time evolution of the state $|\psi\rangle$

$$U = e^{-i\frac{Ht}{\hbar}} \tag{2.3}$$

Where the Hamiltonian, H is assumed to be time independent, and $\hbar$ is Planck's constant. For simplicity, we will use $\hbar = 1$. The evolution of an initial state at time $t = 0$, given by $|\psi(0)\rangle$, is given by:

$$|\psi(t)\rangle = U(t)\,|\psi(0)\rangle \tag{2.4}$$

And $|\psi(t)\rangle$ is the final state at time t. Because it is a closed system evolution in a finite dimensional space, the norm of the vector $|\psi(0)\rangle$ is preserved [13]. Unitary evolution also preserves quantum superposition [142].

Having determined how the closed system evolves, we can also calculate expectation values of observables $\hat{\mathcal{O}}$ at different times:

$$\langle \mathcal{O}(t)\rangle = \langle\psi(t)|\,\hat{\mathcal{O}}\,|\psi(t)\rangle$$

There also exists the possibility that a closed system is subject to external forces, and then the Hamiltonian will become time dependent. When this is the case, the evolution is carried out as a Dyson series through the time ordered evolution operator [61, 13, 48]:

$$U = T_{\rightleftharpoons} e^{\frac{-i}{\hbar}\int_{t_0}^{t} H(t')dt'}$$

This is a unitary operator, or propagator, that acts on the system for a time interval $[t_0, t]$. The operator $T_{\rightleftharpoons}$ here has the two arrow directions in the subindex for use in a general

context. However, one order is selected, depending on the ordering of the product of the propagators. $T_{\leftarrow}$ orders the propagators *chronologically*, i.e. the time arguments will increase from right to left. $T_{\rightarrow}$ is the *antichronological* ordering, where the time argument increases from left to right [61].

An open quantum system will not evolve unitarily. In the later case, there are effects that cannot be described with the formalism above. The dynamics of an open system are usually described with master equations or with dynamical maps. Master equations are a widely used tool[61], however, the focus of this dissertation will be on dynamical maps, which allow for description of system dynamics that have been interacting with a reservoir, bath or environment, without recurring to the perturbative limit. We first look at the properties of the density operator, this is because, although the state vector $|\psi\rangle$ contains all the information about the system, some processes, such as relaxation [53], decoherence and mixed states, which may arise from lack of knowledge of the quantum state in an experiment, are better represented with the density matrix.

2.2 THE DENSITY OPERATOR

The density operator is used to represent the most general state of a quantum mechanical system. It arises from the statistical interpretation of quantum mechanics [61, 120]. If we consider an ensemble of $\mathcal{N}$ identical systems, all characterized by the same Hamiltonian, $\hat{H}$, then the state of each system in the ensemble is given by a normalized vector $|\psi_k\rangle$. Every state vector is defined by the linear combination of the eigenbasis states $|\psi\rangle = \sum_i c_i |\phi_i\rangle$, the density matrix has a standard representation:

$$\rho = |\psi\rangle \langle\psi| = \sum_{ij} c_j^* c_i |\phi_i\rangle \langle\phi_j| \tag{2.5}$$

The elements of this matrix are given by the numbers c_i

$$\rho_{ij} = c_i c_j^* \tag{2.6}$$

When $i = j$, the product $c_i^* c_i = |c_i|^2$ is a diagonal element of ρ and represents a probability that a measurement will yield the state $|\phi_i\rangle$. The off diagonal terms, $c_j^* c_i$, represent the quantum superpositions of the basis states. Therefore, Eq. (2.5) can be written as

$$\rho = \sum_{ij} \rho_{ij} |\phi_i\rangle \langle\phi_j| \tag{2.7}$$

Given an orthonormal set of basis kets $|j\rangle$, the density operator is given by:

$$\rho = \sum_{j} p_j |j\rangle \langle j| \tag{2.8}$$

The p_j represent the probabilities associated to each state $|j\rangle$; a mixed state will be a linear combination of the states $|j\rangle$, and a pure state is one in which only one of the probabilities is equal to 1 and the rest are 0.

The preferred notation in quantum information is in terms of the 2×2 unit matrix and the Pauli spin $\frac{1}{2}$ matrices, since they are the basis for the algebra of qubits.

$$\rho = \frac{1}{2} (\mathbb{1} + \vec{a} \cdot \vec{\sigma}) \tag{2.9}$$

Where the coefficients a_i are the projections along the x, y and z directions of the *Bloch vector*. The Bloch vector is a geometric representation of the states of two-level systems in terms of a sphere of radius 1, called the Bloch sphere, such as the one in figure (2.1) (for higher dimensional systems, this is referred to as the polarization vector, coherence vector, or generalized Bloch vector. See [102, 15, 16, 90, 24, 55, 22] and references therein).

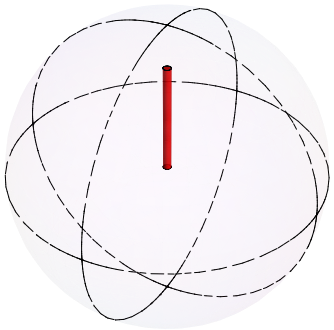

Figure 2.1. The Bloch sphere provides a visual representation of the state of a two-level system.

The coefficents a_i of the Bloch vector are subject to the constraint $\sqrt{a_x^2 + a_y^2 + a_z^2} \leq 1$, for a normalized state; $\mid \vec{a} \mid = 1$ represents a pure state. Any state on the surface of the Bloch sphere is a pure state. A mixed state is represented by a vector with $\mid \vec{a} \mid < 1$. This notation makes it possible to have a visual representation of the quantum state of a two level system at different times when it undergoes time evolution.

In any basis, the density operator is a $n \times n$ matrix, where n is the dimension of the system, and provides the most general picture of a quantum mechanical state [26]. However, not any $n \times n$ matrix represents a quantum mechanical state, and while the properties of the state vectors that generate the density matrix through the outer product should preserve the properties that make it relevant to a physical system, the following subsection will provide the characteristics that must be preserved under any dynamical process (closed or open), such that the density operator represents the state of a quantum mechanical system.

2.2.1 The properties of the density operator

A density operator that represents the state of a quantum mechanical system must satisfy the following conditions [48, 96]:

$$\rho = \rho^{\dagger}, \text{ it is Hermitian,} \tag{2.10}$$

$$\begin{aligned} \rho \geq 0, \quad & \text{it is positive semi-definite,} \\ & \text{i.e. its eigenvalues are non-negative,} \end{aligned} \tag{2.11}$$

$$\begin{aligned} \mathrm{Tr}(\rho) = 1, \quad & \text{it has trace 1,} \\ & \text{i.e. the sum of the probabilities is 1.} \end{aligned} \tag{2.12}$$

The first condition, given by Eq. (2.10), guarantees that the eigenvalues of the density matrix are real, thus experimentally measured quantities are real as well. The second condition, Eq. (2.11), ensures that the eigenvalues are positive. This provides a valid probabilistic interpretation of the density matrix [103], i.e. ensures there are no negative probabilities. The last condition, Eq. (2.12), ensures that the probabilities associated to the basis vectors that span the space of the state of the system sum to one.

The evolution of a density matrix representing the state of a closed system is also unitary process [26]:

$$\rho(t) = U(t)\rho(0)U(t)^{\dagger}$$

That preserves the norm of the basis states and the quantum superpositions. Expectation

values are obtained through the trace

$$\langle \mathcal{O}(t) \rangle = \mathrm{Tr}[\hat{\mathcal{O}}\rho(t)] = \sum_{mn} \mathcal{O}_{mn}\rho_{mn}$$

Before this last section, we reviewed closed quantum system dynamics, however, quantum systems are rarely, if any, completely isolated from the environment. Isolation acquired for experimental pusposes may be costly and difficult as the size of the system increases. Interactions with the environment lead to processes that spoil the unitarity of the system dynamics, and therefore cannot be mathematically described as such. The two main effects arising from the interaction with the environment are: dissipative processes, in which there is an exchange of energy with the environment, and leads to modification of the populations (diagonal terms of the density operator, also known as T_1 type of decay [91]); and decoherence, dephasing, or phase randomization, which involves decay of quantum coherent superpositions (decay of the off diagonal terms of the density operator, also known as T_2 type of decay [142, 91]). Decoherence is a term that has been generalized to describe dissipative processes, however, here the term will be used to define its original context, which is dephasing. A unitary operator does not describe dynamics when these processes occur, therefore the next section will cover quantum dynamics for open systems, focused on dynamical maps (for master equation formalism, refer to [61] and references therein).

2.3 OPEN QUANTUM SYSTEM DYNAMICS

A system, S, that is coupled to an environment, E, will no longer evolve unitarily. The coupling to E gives rise to quantum and/or classical correlations, that spoil the unitarity of the time evolution of S [91].

A valid assumption is to consider that the system and the bath form one joined closed system, $S + E$, that undergoes a global unitary evolution. The final state of this joint system is a pure state [143]. But we are often interested only in the evolution of S. Since

we can no longer describe the evolution of S without taking into account the effects of E on it, we look at the *reduced dynamics of the system*, which provides the density matrix that represents the state of the system after it has interacted with E. It is obtained through the partial trace over the environment E:

$$\rho_S(t) = \mathrm{Tr}_E[\rho_{SE}(t)] = \mathrm{Tr}_E\left[U_{SE}(t)\rho_{SE}(0)U_{SE}^\dagger\right] = \sum_\alpha \lambda_\alpha \zeta_\alpha(t)\rho_S(0)\zeta_\alpha^\dagger(t) \tag{2.13}$$

And the evolution of S, including the effects of its interaction with E, will be fully characterized by the matrices ζ_α [14, 26]. This is called a dynamical map, and will be described in the next section.

2.3.1 Dynamical maps

Dynamical maps are the linear mapping of an initial state in the domain, the space $\mathcal{H}_S$, at time t_0 to a final state in the range, which is the same, or a different (e.g. when it is an assignment map, explained below, or a projection operator), Hilbert space at a later time t.

The dynamical map is required to transform quantum states into quantum states in order to be relevant to physics. Therefore a dynamical map is subject to the following conditions [96]:

1. Is linear $\Phi[p\rho_1 + (1-p)\rho_2] = p\Phi[\rho_1] + (1-p)\Phi[\rho_2]$
2. Is trace preserving $\mathrm{Tr}(\Phi[\rho(0)]) = 1$
3. Is positive $\Phi[\rho(0)] \geq 0$
4. Is self adjoint $\Phi[\rho(0)^\dagger]^\dagger = \Phi[\rho(0)]$

The first condition requires that the map is independent of the initial state of the system [48, 27], and also means that the action of the map can be represented in terms of

its eigenmatrices, $\zeta^{(\alpha)}$, and its eigenvalues, λ_α, as follows [27]:

$$\Phi[\rho(0)] = \sum_\alpha \lambda_\alpha \zeta^{(\alpha)} \rho(0) \zeta^{(\alpha)\dagger} \tag{2.14}$$

The last three conditions guarantee that the mapped final quantum state has trace 1, is positive (has positive eigenvalues) and is Hermitian.

The most general linear mapping is an $n^2 \times n^2$ homogeneous matrix, or superoperator, that acts on the initial state of the system. This superoperator acts on the quantum state of the $n \times n$ density operator rearranged as a $n^2 \times 1$ column vector [48], such that:

$$\rho(t) = A\rho(0)$$

In index notation:

$$\sum_{r's'} \rho'_{r's'}(t) = \sum_{r's'rs} A_{r's',rs}\rho_{rs}(0), \tag{2.15}$$

One could think that any matrix A, with the right dimensions, can be used to map an initial state to a final one in the same Hilbert space, but physics restricts the class of operators A that can be considered dynamical maps. According to [48], the matrix A must satisfy the following conditions

$$\sum_{r's',rs} A_{r's',rs} = (\sum_{r's',rs} A_{s'r',sr})^*, \text{ } A \text{ preserves Hermiticity,} \tag{2.16}$$

$$\sum_{rsr's'} x_r^* x_s A_{rs,r's'} y_{r'}^* y_{s'} \geq 0, \text{ } A \text{ preserves positivity,} \tag{2.17}$$

$$\sum_r A_{rr,r's'} = \delta_{r's'}, \text{ } A \text{ is trace preserving.} \tag{2.18}$$

These conditions ensure that the final quantum state mapped by A is Hermitian, has trace 1 and is positive. However, it should be noted that A may not be necessarily Hermitian.

The characteristics of A are further analyzed by interchanging indices and obtaining another $N^2 \times N^2$ supermatrix B. In brief, the rows of matrix A become block matrices of B, row 1 of A will become the first $n \times n$ block matrix of B, then row 2 is the second one, and so forth. Then the properties of B are [48]

$$\sum_{rr',ss'} B_{rr',ss'} \equiv \sum_{rs,r's'} A_{rs,r's'}. \tag{2.19}$$

The $1 \times N^2$ rows of A become the $N \times N$ block matrices of B. The following conditions are imposed on B so that it represents a physical map:

$$B_{rr',ss'} = (B_{r'r,s's})^*, \ B \text{ is Hermitian}, \tag{2.20}$$

$$\sum_{rsr's'} x_r^* y_{r'} B_{rr',ss'} x_s y_{s'}^* \geq 0, \ B \text{ is positive semi-definite}, \tag{2.21}$$

$$\sum_{r} B_{rr',rs'} = \delta_{r's'}, \ B \text{ is trace preserving}. \tag{2.22}$$

The action of B is not the same as that of A, i.e. not through direct matrix multiplication. The action of B can then be determined by decomposed in its eigenmatrices and eigenvalues and writing the sum:

$$\rho(t) = B\left[\rho(0)\right] = \sum_{\alpha} \lambda_\alpha \zeta_\alpha \rho(0) \zeta_\alpha^\dagger \tag{2.23}$$

Where $\lambda_\alpha \in \mathbb{R}$ are the eigenvalues of B. The Hermiticity of $\rho(t)$ is guaranteed by the restriction given in Eq. (2.20) [26], so that B must be Hermitian. The matrix A is required to transform $\rho(0)$, in vector form, into another Hermitian state $\rho(t)$, but A is not necessarily Hermitian itself.

Complete and not complete positivity

When all of the eigenvalues of B are positive, the map is said to be a completely positive (CP) map (see Ref. [119] and references therein). In this case, the eigenvalues can be absorbed in the eigenmatrices like $\sqrt{\zeta_\alpha}$ so Eq. (2.27) becomes

$$B\left[\rho(0)\right] = \sum_\alpha C_\alpha \rho(0) C_\alpha^\dagger, \tag{2.24}$$

where $C_\alpha = \sqrt{\lambda_\alpha}\zeta_\alpha$.

Eq. (2.24) is sometimes known as the Kraus representation or operator-sum decomposition [39], although it was originally discussed in this context by Sudarshan, Mathews, and Rau [48]. Note that when the system is closed, the map is completely positive, and there is only one C_α, which is the unitary operator $U(t)\rho(0)U^\dagger$ [26]. Thus we can see why dynamical maps are the most general representation of a quantum dynamical process.

This CP map can also be derived from the reduced dynamics of a state that is initially uncorrelated from the bath:

$$\rho(0) = \rho_S(0) \otimes \rho_E(0)$$

Expressing the initial state of the bath as $\rho_E = \sum_i \nu_i \left|i\right\rangle \left\langle i\right|$ and taking the trace over E:

$$B\left[\rho(0)\right] = \sum_{ij} \left\langle j\right| U(t)\rho(0) \otimes \nu_i \left|i\right\rangle \left\langle i\right| U^\dagger(t) \left|j\right\rangle = \sum_{ij} \nu_i \left\langle j\right| U(t) \left|i\right\rangle \rho(0) \left\langle i\right| U^\dagger(t) \left|j\right\rangle \tag{2.25}$$

Then we define $C_\alpha = \sqrt{\nu_i} \left\langle j\right| U(t) \left|i\right\rangle$, and provided that all the ν_i are positive, we obtain Eq. (2.24).

If at least one eigenvalue is negative, but the map still transforms a positive ρ into another positive ρ, the map is non-completely positive (NCP). Reduced dynamics have been restricted to satisfy the condition of complete positivity because their interpretation is

not completely understood and also because CP maps preserve positivity even if the size of the Hilbert space is increased.

Pechukas was the first to demonstrate in 1994 that reduced dynamics do not need to be completely positive. He showed that complete positivity constrains a system to initial separable product states $\rho_{SE} = \rho_S \otimes \rho_E$, where ρ_E is a fixed state of the bath [110, 1]. Jordan, et al. demonstrated that entanglement in the initial state of the system can lead to non-completely positive maps, yet the map is still positive [134].

Moreover, non-completely positive (NCP) maps have been measured experimentally using quantum process tomography (QPT) [75, 3], which has caused the specifics of QPT to be questioned [28]. But the possibility that a map which is not a completely positive map can transform a valid quantum state into another state that satisfies the conditions in Eqs. (2.10), (2.11) and (2.12), has brought a great deal of interest in studying the conditions for complete positivity, the main question is: what kind of correlations result in a NCP map? This is in addition to the interest in NCP maps due to the partial transpose as an indicator of entanglement [11, 98].

To differentiate the initial state from a simply separable one, we introduce the correlation matrix $\rho_{corr}(0)$:

$$\rho(0) = \rho_S(0) \otimes \rho_E(0) + \rho_{corr}(0) \tag{2.26}$$

The element $\rho_{corr}(0)$ contains all the correlations, but its not a quantum state [13]. It satisfies $\mathrm{Tr}_S \rho_{corr}(0) = \mathrm{Tr}_E \rho_{corr}(0) = 0$, since is traceless (it must be to preserve the properties of ρ). With an initial state of the form of Eq. (2.26), one can write the dynamical map as a sum of two contributions:

$$\rho(t) = \Phi\left[\rho(0)\right] = \sum_\alpha C_\alpha \rho_S(0) C_\alpha^\dagger + \mathrm{Tr}_E[U(t)\rho_{corr}(0)U^\dagger(t)] \tag{2.27}$$

The first part is CP and depends on the global unitary and the initial state of the bath. The last term, however, depends on the initial SE correlations [13]. A quantum system that interacts with the environment before our prescribed $t = 0$ can be described by completely positive dynamics if the environment does not re-act on the system [26], i.e. the coupling is weak and/or the initial state is in a particular form [110]. More broadly speaking, according to [27] if the initial state has only classical correlations with the environment, then this is a sufficient condition for the dynamical map to be completely positive. The nature of the correlations is defined in terms of the"quantum discord", which is a measure of the "quantumness of correlations" [107]. Quantum discord vanishes when the correlations are classical and it's a maximum when there is entanglement. But more specific detail on the nature of initial correlations is provided by the authors of [84]. They state that correlations which are Markovian satisfy

$$\mathrm{Tr}_E \left[U(t)\rho_{corr}(0)U^\dagger(t) \right] = 0$$

for different times, thus providing CP dynamics for Markovian models.

Shabani and Lidar demonstrated that vanishing quantum discord is not only sufficient, but a necessary condition for complete positivity [131], this means that quantum correlations should yield NCP dynamics *every time*. However Brodutch, et al. [4], provide a counter-example of an initial state with non-vanishing quantum discord that contradicts this last statement. So the question of which types of initial correlations result in a NCP map remains open. Why is the initial state so important in determining this? This is a question that can be answered by looking at the map as a composition of maps.

2.3.2 Composition of dynamical maps: Assignment maps and consistency

Just like a function can be a function of other functions, a dynamical map can be a function of other maps. Pechukas, in [110], introduced the concept of the assignment map,

Λ. Λ is the map that assigns the state of S to some state in the larger space SE [110, 27]. The assignment map is one of three maps that compose the complete dynamical map; the other two are the trace with respect to the bath, $\mathcal{T}_E$ and the global unitary transformation U_{SE}, therefore:

$$B = \mathcal{T}_E \circ U_{SE} \circ \Lambda \tag{2.28}$$

where $\circ$ is the composition function (see Appendix 5.1). So then Eq. (2.13) is written as

$$\Phi[\rho_S(0)] = \rho_S(t) = \mathrm{Tr}_E \left\{ U(t)\Lambda[\rho_S(0)]U^\dagger(t) \right\} \tag{2.29}$$

Because the unitary and the trace are linear and completely positive, the positivity or non complete positivity should arise from the assignment map, Λ [28, 84, 4]. The assignment map is the one that contains information about possible correlations in the initial state. Alicki [115], defines the following conditions on the assignment map:

1. Linearity $\Lambda[p\rho_1 + (1-p)\rho_2] = p\Lambda[\rho_1] + (1-p)\Lambda[\rho_2]$, where $p \leq 1$
2. Consistency $\mathrm{Tr}_E[\Lambda\rho(0)] = \rho(0)$
3. Positivity $\Lambda[\rho(0)] \geq 0$

According to Alicki there is no general definition for the reduced quantum dynamics beyond the weak coupling regime , therefore, when the system is in an initially correlated state with the environment, linear assignment maps have no unique definition [28], and linearity would only be preserved for states that are invariant under the transformation [115]. Pechukas concurred with Alicki on giving up linearity for initial states that are not weakly coupled to the environment [1]. However, Rodriguez-Rosario et al. examine the assignment maps and argue against giving up linearity by noting that the assignment maps can be linear if the conditions of consistency or positivity are relaxed, and favor relaxing the positivity condition [28]. Giving up complete positivity means that the assignment

map that transforms a state in S to a state in SE is NCP, even if the state in SE is positive, and this will cause the dynamical map B to be NCP.

Giving up consistency means that the same initial state is not obtained after tracing over environmental degrees of freedom, it refers to errors in the preparation of initial states; this is particularly possible in quantum process tomography experiments. When there are errors in the preparation (such as unwanted correlations with E), there can be a loss of consistency and therefore in a NCP map. But according to [28] it is undesirable to give up consistency because it can result in non linear maps, due to the dependence on the initial state.

Why is complete positivity relevant? the answer is because it guarantees positivity of the final density operator. Also, the map will remain CP when it is extended to higher dimensions. However, CP maps are restricted to a reduced class of states, which excludes correlations with the environment and therefore many realistic physical situations.

It is important to study dynamical maps beyond the initially separable state assumption. Dynamical maps directly characterize the dynamics of quantum systems [101], and more importantly, outside the Markovian regime [12, 84]. Modelling dynamics of initial states that are not uncorrelated from the environment is becoming increasingly important. Part of the present work consists of studying a quantum simulation algorithm developed by Ortiz et al. [56] in the presence of errors and correlations in the initial state of the system. The open quantum system dynamics are described with dynamical maps [105], mainly to observe the effects of errors in the preparation of initial states, which are key to successful quantum simulation experiments.

CHAPTER 3

QUANTUM SIMULATORS

3.1 QUANTUM SIMULATORS

3.1.1 Introduction

Most of the results presented in this section have been published in [105].

Numerical simulations allow us to further understand experimental as well as analytical results, but more importantly, they allow us to simulate physical problems for which exact models are difficult. This is the case for many problems in high energy physics, atomic physics, condensed matter,cosmology, biology and quantum chemistry, among others. It is known that in the case of quantum mechanics classical simulation becomes intractable for systems with more than 50 particles [74]. This is because the dimension of the Hilbert space increases exponentially with the size of the system[130, 32, 121, 129, 70, 56, 123, 122, 30, 76, 31, 80, 85], and that requires more computational resources than those currently available[85]. Some problems in which computational power is an issue include: the quantum many-body problem, high temperature superconductivity and quantum field-theories [20, 125, 83].

In a classical simulation, the state of an N 2-state particle system is represented by a 2^N vector; simulating this system classically implies storing 2^N complex coefficients to represent that state as a linear combination of the 2^N orthogonal states that span the Hilbert space of the system. Moreover, time evolution makes it necessary to perform operations with those coefficients in order to predict quantities of interest. Computationally, this problem becomes intractable when the number of two level particles exceeds 50 [109, 74]. The amount of memory required to do this exceeds a terabyte, which would occupy the entire memory space available of some currently existing classical computers.

Richard P. Feynman proposed in 1982 the idea of a "quantum simulator", i.e. a

quantum system that could be used to simulate another quantum system. A quantum simulator could be a collection of spin $\frac{1}{2}$ particles that can be manipulated at will through external controls (e.g. lasers)[74], such that the interactions between them are modified to simulate the evolution of another system of interest. Then the desired quantities would be extracted by performing measurements on the simulator. This type of device can perform the task much more efficiently than a classical computer [124], because it only requires N qubits to store the state of N spin $frac12$ particles; and this alone provides an exponential reduction in the amount of computational resources required [126, 50, 74].

Evolution of the system, however, requires a $N \times N$ unitary operator. This takes an exponential amount of resources, even in a quantum simulator. Nevertheless, Lloyd demonstrated in 1996 that this problem can be overcome by evolving the system in small, discrete time steps; and by turning on and off the correct sequence of Hamiltonians, a quantum simulator can be programed to mimic any evolution of quantum systems subject to local interactions [126].

In addition, a quantum simulator behaves according to the laws of quantum mechanics, just like the system it is built to emulate [74], and this means that they would provide insight on quantum phenomena that may not be available otherwise. Quantum simulators might also help overcome the sign problem in Quantum Monte Carlo algorithms for fermionic systems or the exchange-correlation functionals in Density Functional Theory [56, 78].

The possibility of finding answers to problems that are intractable using classical computers has brought a great deal of interest in the field of quantum simulations. A large portion of the existing theoretical work is devoted to the development of algorithms for implementation on specific existing devices which perform as simulators [56, 145, 50, 127, 128, 62, 72, 85, 97, 70, 68, 18, 63, 82, 2], and some simulations have been carried out experimentally [73, 76, 146, 71, 29, 118, 117, 99].

Nevertheless, a quantum simulating device is, after all, a quantum system, and its

interaction with the surrounding environment is unavoidable. It is therefore necessary to study how the interactions affect it, whether they can be included in the simulation or if error correction is necessary and if so how. Noise in quantum systems can cause discrepancies in the output of a quantum simulation, affecting the final result in an undesirable manner [88].

The following subsections provide a brief review of advances on the realization of quantum simulators. The present work is focused on a specific algorithm, but an introduction to these devices and how they operate provide the necessary background to understand the problem.

3.2 EXPERIMENTAL IMPLEMENTATION OF QUANTUM SIMULATIONS

Quantum simulation is one of the motivations for building a fully functioning universal quantum computer. A quantum computer would serve as a universal quantum simulator, in the sense that it should be capable of simulating any other quantum system [36, 67]. Universal quantum computation relies on a universal gates that act on a collection of two-state systems [38, 79, 114]. The state of the quantum system of interest is represented with qubits [67]. And operations are performed as a stroboscopic sequence of quantum gates to mimic any unitary transformation. Building a quantum computer though requires controlling particles for long periods of time and measuring final states, both with high precision, which requires a large number of quantum gates [88]. And during these operations the fidelity of the computation will be affected by interactions with the surrounding environment and with other particles in the system [135]. This causes both evolution and measurement to lose precision. Since these errors are not yet able to be overcome, it will take some time before a fully-functioning fault-tolerant quantum computer can be built.

A quantum simulator can also be a system composed of a finite number of particles

that can be manipulated with external controls. In these systems the Hamiltonian of the system will be directly mapped onto a many body Hamiltonian that constitutes the simulating device. Given an initial state $\Psi(0)$, time evolution is performed by inducing interactions between the particles, and then properties of some final state $\Psi(t)$ can be studied [74]. These devices operate continuously in time instead of through discretized unitary transformations, as a quantum computer does. Universality in these devices means finding a many body system that can be engineered to simulate any other many body Hamiltonian, though, just as with a quantum computer, is difficult to achieve, therefore, there are no universal quantum simulators available.

Fortunately, recent experimental advances in quantum control techniques are reaching highly sophisticated levels for many systems; these include: ultracold atoms, ultracold Fermi gases, ion traps, quantum dots, atoms in optical lattices, coupled cavities, photons, superconducting qubits and NMR devices
[67, 43, 77, 50, 76, 80, 85, 146, 99, 71, 127, 2, 66, 109]. This, in addition to the availability of universal gates to many physical systems [109], has made it possible to design smaller scale quantum systems as specialized quantum simulators in order to study characteristics of specific systems of interest, such as Fermi-Hubbard models [65].

Because both types of devices have been proposed as universal quantum simulators, and specialized ones are available with both operation schemes described above, there exist two main classifications of quantum simulators:

1. The Digital quantum simulator (DQS) [67], which includes those quantum simulators which operate under the same principles a quantum computer would [67], and evolution of the system is carried out through stroboscopic sequences of quantum gates to simulate a unitary evolution.

2. The Analog Quantum Simulator (AQS) [67, 135, 109], which refers to the device which involves direct mapping of the Hamiltonian of interest onto the Hamiltonian of the controllable system and continuous time operation [67], which is a Hamiltonian

with "always on" interactions [109], and evolution is carried out continuously in time by modifying these interactions. These were initially referred to as Specialized Quantum Simulation (SQS) [69, 95], because they were systems designed to simulate very specific models, but the possibility of universality and the fact that DQSs can be used as specialized quantum simulations, calls for a broader definition.

Further sub classification is provided by Hauke, et al. in [109], who identify three subtypes of simulators in each category according to their universality and applicability. The details of these will be provided next.

3.2.1 Analog and digital quantum simulators

In this section we will go over the subtypes of quantum simulators in each category. Hauke et a. [109] identify each subcategory according to their universality and purpose.

1. Analogue Quantum Simulators:

    - Universal Analogue quantum simulators (UAQS): Which are controllable many-body Hamiltonians that can be used to represent any Hamiltonian evolution; mapping of systems of interest onto these Hamiltonians is done with specifically designed unitary control sequences; the unitary transformations in these control sequences are one or more particle operations to map the Hamiltonian of interest onto the one in the UAQS. Universality for AQSs is concerned with the Hamiltonians can be used as simulators and to what degree of accuracy they can represent other systems. This has been the subject of extensive research in recent years [35, 79, 113, 112, 111, 94, 100, 8, 6, 7]. Work by Childs characterizes the family of two-qbit Hamiltonians and determined conditions under which they fail to be universal [7]. Berry et al [41] considered the simulation of more general sparse Hamiltonians, which are not necessarily representative of a system composed of tensor products of subsystems. Instead,

they have a fixed number of nonzero elements per row. Their algorithms improve the simulation time by reducing it to almost linear. But, these kinds of Hamiltonians are more applicable to quantum algorithms than to physical systems [83]. More complex non-sparse Hamiltonians are analyzed by Childs, et al. [6] and their results show that there is no general algorithm for their simulation; finding control sequences and calculating their efficiency can be an extremely difficult task [6, 83]. Dur et al. [141] studied the possibility of using "always on" Hamiltonians for universal quantum simulations for which time evolution would be carried out through a Trotter decomposition, but found them to be inefficient for this purpose due to noise and timing errors [141, 109]. Some theoretical universality questions still remain for very specific systems, but many have been already answered [83]. Although there exist some proposals for implementation [51], there is no universal AQS available, mostly due unsolved controllability issues arising from scaling of the system.

- Non-Universal Analogue quantum simulators (nUAQS), which are currently the most widely available type of quantum simulators. These are Hamiltonian simulators that operate continuously in time, built to specifically carry out the quantum simulation of certain systems of interest [109]. Giving up universality allows the experimentalist to use a system that will have a Hamiltonian similar to that of the system that will be simulated, something that is desirable for accuracy of the results. There have been many theoretical proposals [56, 122, 50, 30] as well as experimental realizations[80, 54] for nUAQS. Although not universal, these types of simulators promise to provide answers to problems that have no known analytical solution and take more than the currently available computational resources.

- Open-System Analogue quantum simulators, which can be any non universal analogue simulators, but in this case the purpose is to simulate the appropriate

master equation [83]. In the Markovian regime, the system would simulate a Linblad master equation for a density operator. There exist some algorithms, which propose to include the environment as part of the experiments, such as those designed by Mostame et al. and Wang et al. [63, 128], however, these algorithms are designed to observe non-Markovian effects, therefore, cannot be described with Linblad operators. And since the environment is included as a part of the total system, these most likely fit in the category of nUAQSs. Experimentally, Barreiro, et al. proposed an ion trap simulator to emulate open quantum systems of up to five qubits [80]. As opposed to designing dissipative gates, including the environment as part of the joint system could provide valuable information about non-Markovian dynamics. The Markovian approximation used to model open quantum system dynamics provides mathematical simplicity, but there is an increasing demand for models that include initial correlations/interactions [84, 26], and studying noisy quantum simulations may help provide insight about the effects of interactions and possible memory effects.

2. Digital Quantum Simulators:

   - Universal Digital quantum simulators (UDQS). The quantum simulator proposed by Lloyd in [126] has been defined as the universal digital quantum simulator.A universal DQS is, in principle, a universal quantum computer. But the availability of systems for which a universal set of gates is available (such as ultra cold trapped atoms and ions, superconducting qubits, etc.), have made it possible to experimentally realize a UDQS without having to build a quantum computer [109, 129, 36, 73, 21]. These types of devices are expected to be the most reliable types of simulators, because universal error correction is available to them. However, errors can be introduced by the Trotter decomposition of the

unitary evolution, and error correction can increase simulation time, reducing the efficiency.

- Non-Universal digital quantum simulators: these are special-purpose digital quantum simulators that operate with a non-universal set of gates [64]. These can be realized by limiting the set of universal gates on systems to which they are available, and thus obtain special purpose digital quantum simulators. Once more, specifically designing a device to simulate a quantum system may be advantageous in the sense that the simulation may be more accurate. However, according to [109] universal error correction is not guaranteed for these type of simulators.
- Open-System digital quantum simulators: These are simulators that operate under a set of universal dissipative gates, realized by tracing out ancillas. In the simplest case, these gates correspond to Linblad superoperators, which represent Markovian dynamics [109].

The availability of non universal analogue and digital quantum simulators makes it possible to experimentally study problems of interest in the present day [51, 77, 108, 81, 80, 73, 76, 146, 29, 118, 18, 117, 21, 54]. There should be, nevertheless, some caution in their use.

Isolation has been achieved for a relatively small number of particle, thus enabling small scale quantum computing [74, 80]. But the purpose of realizing quantum simulators is to model the dynamics of systems which are not efficiently simulatable in a classical computer, i.e. for many body systems that are composed of more than 50 particles.

Dynamical decoupling [136] can be used to avoid noise arising from interactions with the environment, but this task is non trivial, and even if it is accomplished, there exists the possibility of interactions between the particles of a quantum simulator. A quantum state can be prepared ideally, but if some time passes, there can be some unwanted interaction with other parts of the system or with the environment. And also, due to the probabilistic

nature of quantum systems, the experiment may need to be realized many times, a factor that could diminish the efficiency of the simulation. All these factors should be considered in AQSs because error correction and fault tolerance are not available to them [109]. Even though it has been suggested that noise suppression may not be as necessary for a An additional factor is in using AQSs is the efficient design of control sequences, which is a computationally hard problem [83, 44, 94, 56, 123, 122].

Now, it has been mentioned that the simulator should have a Hamiltonian that is similar to the Hamiltonian of the simulated system. To better understand why, we refer back to the processes associated to the interaction of a quantum system with the environment: decoherence and dissipation. The term decoherence is used here in its original context, which is the process of decay of quantum coherence. The term has been generalized to include dissipative processes [91], and to define noise in quantum systems in general. But the distinction is made here for the definition of the timescales.

The relaxation time, τ_{rxn}, is the time it takes for the system to undergo a loss of energy to the environment, which affects the populations (diagonal terms) of the density operator. The decoherence time τ_{dec}, is the time it takes for the coherence to become less than one (decay of the off-diagonal terms). to last for up to 300 fs at room temperature. The ratio between these two time scales determines whether one or the other processes dominates the open system dynamics. In many systems τ_{dec} is much smaller than τ_{rxn}, so the dominating process is dephasing. In this sense it is easy to see that the simulator and the system of interest should have similar timescales.

3.3 QUANTUM SIMULATION PROCEDURE

The main task of a quantum simulator is the time evolution of a system governed by a Hamiltonian, H [44, 83]:

$$|\Psi(t)\rangle = e^{(-iHt)} |\Psi(0)\rangle \tag{3.1}$$

Where $\Psi(t)$ is the wave function representing the state of the quantum system at a time t, and for simplicity $\hbar = 1$. The basic quantum simulation procedure thus has three steps [106, 122, 67]: initial state preparation, evolution of the quantum system, output and measurement of a physical property of interest on the final state. There exist more than one method to implement each of these steps, and will be described in more detail in the following subsections.

3.3.1 Initial State Preparation

In this first stage, the state of the system is mapped onto that of the quantum simulator. It is an extremely important step, because the final state depends on it, and errors in the preparation lead to deviations from expected results.

The main preparation methods are listed below:

1. Zalka's method. In [33], Zalka proposes to map the discretized wavefunction onto a qubit register of length L, in which the norm, l, of the wave function is 'split' L times as follows

$$|\psi\rangle = \sum_{n}^{2^L-1} \langle n| \left|\psi\left(n\frac{l}{2^L}\right)\right\rangle |n\rangle \tag{3.2}$$

   Where the basis states $|n\rangle$ are assigned by the binary representation of n. And this is subject to periodic boundary conditions, $|\psi(x+l)\rangle = |\psi\rangle$.

2. *Direct Preparation*, which includes all methods for state preparation of quantum registers [83]. Some methods involve the use of quantum gates and/or quantum algorithms, such as Grover's algorithm [56, 83].

3. *Adiabatic Evolution*, in which a system is evolved adiabatically from the ground state of an initial Hamiltonian to the ground state of a final Hamiltonian:

$$H(t) = (1 - s(t))H_0 + s(t)H_f, \tag{3.3}$$

where $s(t)$ is a time dependent monotonically increasing function which determines the speed of the evolution. H_0 is the starting Hamiltonian, and H_f is the Hamiltonian whose ground state we want to use as the initial state of a simulation. In the scheme of quantum computing, as well as in some quantum simulations, the ground state of H_f is the desired solution to the problem [49, 78, 72], but it is easy to see that this is a useful method to prepare an input state [83]. The rate $s(t)$ will depend on the energy gap between the initial ground state and the excited states of the final Hamiltonian [8, 10]. When the gap is larger, the evolution can be performed in less time [83].

4. *Preparation by thermal equilibrium*, in which the system is in contact with a bath that is in a state of equilibrium at a certain temperature; system and bath are allowed to interact for a certain amount of time, after which the bath is reset to the equilibrium state again. Then the procedure is repeated until the system is in the equilibrium state for that temperature [17, 83]. States prepared by thermal equilibrium are very useful for problems in statistical mechanics [69], but have also been used for quantum computation problems [5]. Algorithms that use thermal equilibrium as state preparation for the calculation of thermal rate constants, are a problem of key interest in chemistry [42, 97].

3.3.2 Evolution of the Quantum System

The main difference between DQSs and AQSs is the manner in which the evolution of the quantum state is realized.As stated before, time evolution in a DQS is carried out through a Trotter decomposition, which is a sequence of unitaries that act on smaller size subsystems of the total system for short periods of time. This translates into a stroboscopic application of quantum gates that simulate, in principle, any unitary operator [109]. Time evolution in an AQS, on the other hand, is realized by modifying particle-particle interactions in the "always on" Hamiltonians to evolve the system continuously in time.

Trotter decomposition

Lloyd proposed to carry out the unitary evolution through a Trotter decomposition because the exponential size of the unitary generated by a Hamiltonian could require exponential resources [126, 50, 83]. But also because this formula can be used even for Hamiltonians which do not commute with each other. In this scheme the total Hamiltonian of the system, H, is represented as a sum of n Hamiltonians H_j, that act on smaller subsystems of fixed size ℓ:

$$H = \sum_{j=1}^{n} H_j \tag{3.4}$$

The quantity ℓ is independent of the total system size, N; and it represents the maximum number of nearest neighbors. The number ℓ should remain constant even though N increases, this guarantees that the interactions in the system remain local [83, 6].

In this notation, the entire system is represented as a tensor product of smaller subsystems [41]. The maximum number of terms in the sum n is given by the distribution $\binom{N}{\ell} < N^{\ell}/\ell!$, which implies a polynomial increase of n as N grows [83], not exponential, and therefore only a polynomial number of resources is required [126, 50, 83].

Lloyd also classified the set of operations to carry out evolution in quantum simulators in two:

1. Operations that almost preserve coherence, which are necessary to simulate closed systems subject to Hamiltonian dynamics.

2. Operations that do not preserve coherence, which correspond to open system evolution described by super operators or master equations [126, 83].

Coherence-preserving operations involve turning on and off a set of Hamiltonians $H_1, H_2, ...H_n$ in a controlled manner to carry out a unitary evolution $U = e^{-iHt}$. The total evolution time t is divided into Δ small discrete time steps, and each step is approximated with the Trotter decomposition [83]:

1. Iterations $|\Psi_{j+1}\rangle = U_{\frac{t}{\Delta}} |\Psi_j\rangle$

2. Loop $j = j + 1$ until desired time of evolution is achieved $j\frac{t}{\Delta}t \geq t_f$

If Δ is chosen to be sufficiently large, the dynamics have more controllability and the amount of error is small [126, 78]. Then the unitary operator is carried out as follows:

$$e^{iHt} = (e^{iH_1\frac{t}{\Delta}}e^{iH_2\frac{t}{\Delta}}...e^{iH_n\frac{t}{\Delta}})^{\Delta} + \sum_{i>j}[H_i, H_j]\frac{t^2}{2\Delta} + \cdots, \tag{3.5}$$

An efficient simulation requires that the number of operations performed increase polynomially as $\left(\frac{1}{\delta}\right)$, where δ is the accuracy. Brown, et al. [83] explain the calculation of an upper limit to the efficiency of the Trotter decomposition by allowing the upper bound on the size, ℓ, of the subsystems to be given by the quantity g. The n individual Hamiltonians act on the subsystems of size ℓ. Now, say the size of Hamiltonian H_j is g_j, and $g_j < g$, then g_j^2 operations are necessary to simulate the unitary generated by H_j; and H_j will be simulated in time Δ. This limits the maximum number of operations required to simulate the total e^{-iHt} to $\Delta n g^2$ [83]. Since the error is inversely proportional to the number of time slices as $\epsilon \propto t^2/\Delta$, the number of operations in this algorithm can be calculated as a function of $t^2 n g^2/\epsilon$, and since n scales polynomially with N, then the simulation algorithm is considered efficient [83].

The second kind of operations, those that do not preserve coherence, and are not unitary. These correspond to reduced quantum dynamics of the system after tracing out environmental degrees of freedom. The evolution is described by dynamical maps [126, 37, 83],

$$\mathcal{B}[\rho_S] = Tr_E[W\rho_s \otimes \rho_B W^{\dagger}]. \tag{3.6}$$

According to Lloyd, there is no need to simulate the environment in its totality, but only the effects of the environment that may be relevant to the system. But if the environment is small enough and local, it can be simulated and the evolution of the global unitary carried out by Trotter approximation. A dynamical map can then be obtained to describe

the reduced dynamics of the system after tracing out environmental degrees of freedom, and it should preserve any relevant memory effects.

Evolution by continuous operation

Time evolution in AQSs, on the other hand, is not carried out as a Trotter decomposition, but rather they operate continuously in time. Hamiltonian simulation in the AQS setup is done by increasing the always on interactions present in the Hamiltonian of the system to obtain a final Hamiltonian and, by doing so, simulate the dynamics of many body systems.

Adiabatic quantum simulators can also be used to simulate a system and obtain quantities of interest, in particular when studying the gap between the ground and first excited states [145], especially in the vicinity of a quantum phase transition. In the later case, adiabatic evolution can be used to prepare a state that is a superposition of the ground and first excited states, which then is evolved adiabatically and information is extracted by phase estimation algorithms. The adiabatic approach has been shown to be equivalent to the circuit model in power, but its physical implementation can be quite different.

The evolution of an adiabatic simulator is carried out in the same manner as the state preparation procedure described before, when the ground state of the target Hamiltonian is the quantity of interest. Adiabatic quantum simulators can be classified as AQSs due to their mode of operation, but they do not require a designed control sequence to perform a simulation [78].

3.3.3 Output and measurement of a physical property of the final state

The final step of the simulation is the extraction of the necessary information from the resulting quantum state. We require

$$\left\langle \Psi(t_f) \left| e^{-iHt} \right| \Psi(0) \right\rangle \geq 1 - \delta, \tag{3.7}$$

where δ is the non zero level of accuracy [106]. Projective measurement is not an ideal method. It would alter the final state and provide a limited amount of information. Moreover, to achieve accurate results, the experiment must be carried out N times, with the same initial state. The efficiency of such procedure can only improve as $1/N$ [52].

Many measurement techniques are based on parameter estimation methods [52]. Brown, et al. identify the measurement techniques according to the quantities of interest they are expected to obtain [83].

- Phase estimation algorithms, which are used to obtain energy gaps between ground and first excited states. After performing a unitary evolution on an initial state $|\psi(0)\rangle$, which is an eigenstate of U, the final state will have an eigenvalue $e^{i2\pi\phi}$. The phase, ϕ is obtained by performing an inverse quantum fourier transform (QFT) [116]. This phase difference is proportional to the energy gap between the ground and first excited energy states [83, 144]. Another method to obtain an estimate of this phase difference is by measuring the final state $|\psi(t)\rangle$ using an operator $\hat{O}$, such that;

$$\langle \psi_{ground} | \hat{O} | \psi_1 \rangle \tag{3.8}$$

  Where $|\psi_{ground}\rangle$ and $|\psi_1\rangle$ are the ground and first excited states, respectively. Then the phase difference is extracted by using a classical Fourier transform. This provides an energy spectrum with peaks where the gap and zero are located [88, 83]. This method is particularly useful if an adiabatic quantum simulation has been performed.

Abrams and Lloyd's propose an algorithm to calculate the eigenvalues and eigenvectors of a Hamiltonian H based on phase estimation. The entire procedure describes a quantum simulation, but its necessary to describe it in order to specify the details of the procedure followed to extract the relevant data. Initialization consists on preparing l qubits in a register in a state V_a which is an approximation of an actual eigenstate V of H; in terms of the eigenvectors of H:

$$|V_a\rangle = \sum_k c_k |\phi_k\rangle \tag{3.9}$$

m additional qubits in the register are prepared in the $|1\rangle$ state (spin down, for spin $\frac{1}{2}$ particles), and are labeled the index qubits. Then the total state of the register is

$$|\psi\rangle = |1\rangle |V_a\rangle \tag{3.10}$$

A $\frac{\pi}{2}$ rotation is performed on each of the index qubits, so that the state becomes

$$|\psi\rangle = \sum_j |j\rangle |V_a\rangle \tag{3.11}$$

Then after V_a has been evolved with the unitary operator e^{iHt}, it should be in a linear combination of the $|\phi_k\rangle$ eigenstates with eigenvalues $e^{i\theta t}$. Then a quantum Fourier transform is performed on the index qubits to obtain these phases, and therefore the eigenvalues of H [45]. The accuracy of this procedure is inversely proportional to the overlap $|\langle V_a \mid V\rangle|^2$, which should not be exponentially small.

- Indirect measurement using an ancilla. which was proposed by Somma et al. in [122]. In this scheme, an ancilla qubit is prepared in a specified initial state and then is allowed to interact with the simulated system. At the end of the simulation, a measurement is performed to obtain some quantity of interest.

Somma et al. focus on the evaluation of the time and/or spatial correlation functions, where the ancilla is measured after performing operations with time evolution or translation operators [122]

3.4 UNSOLVED PROBLEMS WITH QUANTUM SIMULATIONS

The first problem is scalability. Increasing the system size decreases its controllability. When Lloyd proposed his method, he limited the efficient simulation to local Hamiltonians. A Hamiltonian which does not satisfy this condition may require $\tilde{N}^2 = 2^{2\times Nd}$ gates per time step to simulate its evolution [50]. This translates into an exponential number of resources to perform the simulation of an arbitrary unitary operator. To overcome this problem, Pritchett et al. have suggested a trade between the polynomial reduction of resources for a reduction in simulation time [50]. Also recent work by Papageorgiou and Zhang makes use of higher order splitting methods which increase the number of exponentials but result in speedups when performing the simulation [9].

Scaling of the system also has implications for the efficiency of the simulation. The amount of error scales as $1/\epsilon$, so, for small ϵ, the number of required resources increases dramatically [135, 88, 83], making error correction necessary, which in turn results in increased simulation time.

Error correction though, is not available for AQSs [109], and scaling these simulators also decreases their controllability. The extent to which we can trust the result of a simulation using an AQS is a question that remains open. Error correction methods are not developed for these kind of simulators. Quantum control has been improved for certain systems, but is usually limited to a few particles [109].

Noise, either in the form of gate errors, interactions between the particles of the simulator, or from interactions with the environment, is another contributing factor. It was initially suggested that decoherence in quantum simulations may not need to be treated in the same strict sense as in quantum computation [126]. However, the interactions of the

simulator with the bath may not be the same as those of the system of interest. Error-correcting codes can be used for DQSs [132, 133, 34, 58, 59, 57], decoherence free subspaces [148, 93, 47, 87, 86, 92] (see also [91, 25] for reviews) and dynamical decoupling [136, 19, 46, 137, 147, 140, 139, 138, 40, 23, 43, 60], may help suppress noise in both types of simulators. An example of error prevention was given by Wu and Byrd in [144], where they show that several algorithms and observables have a robustness to errors when quantum tomography was used to extract data.

In the case of DQSs, the Trotter decomposition can introduce additional noise [56, 31], and can also increase the simulation time in the sense that the number time steps must be increased to achieve a higher degree of precision, and this may not be the most efficient solution.

Other problems in quantum simulations can be caused by errors in the initial state preparation and measurement. In the latter case, its mostly because the amount of information measurement provides is limited. Preparation, on the other hand, is important, since the final state depends on the evolution of the system but also on the initial conditions. For example, preparing ground states may result in a combination of the ground and first excited states when the energy gap between them is small. Experimentally, two different state preparation methods may not yield the same result and can have a profound effect on the outcome [89].

Interactions with other particles in a quantum simulator, whether or not they are thought of as the bath, are a central subject in the present work. We study the effects of errors in the preparation of the initial state and see how the affect the outcome of the simulation. And because the simulator is treated as an open quantum system, we also look at the dynamical maps that describe the evolution of the different initial states. The purpose of observing the effect of errors in the initial state is to obtain information about the types of initial correlations that yield NCP maps.

CHAPTER 4

A QUANTUM SIMULATION WITH NOISE AND DYNAMICAL MAPS

4.1 BACKGROUND

Lloyd suggested that suppressing noise in quantum simulations is not as important as it is for quantum computation [126] and in fact may be used to simulate the interaction with the environment of a system of interest [67]. However, as mentioned before the manner in which noise affects the simulator may differ from that of the system of interest. Even in cases where the bath is engineered as part of the experiment [128], it might be useful to suppress the noise from interactions with the real environment or the quantum simulating device, or to study their effects so they can be identified in the final result. In any scenario, errors need to be minimized [67, 31, 109] to achieve accurate representation of a system of interest. The degree to which noise from the environment or the device should be included in the simulation depends on the systems being used and whether or not these effects are relevant.

In order to study the effects of unwanted noise in a quantum simulation, we selected an existing algorithm that could be simulated in a NMR device to observe the dynamics of different initial states for a closed and open quantum system. To further study the effects of interactions, we also calculated the dynamical maps that describe the evolution of different initial states. The purpose is to observe which initial conditions would lead to non complete positivity, and under which conditions the dynamics can only be represented with an NCP map.

4.1.1 Quantum Algorithm for Simulation

Ortiz, et al. proposed an algorithm for the quantum simulation of the one-dimensional Fano-Anderson model [30]. This model consists of an impurity with energy ϵ surrounded by a ring of n spinless fermions, which have energies ε_{k_i}. The fermions interact with the

impurity, which is also a spinless fermion, through a hopping potential V. The diagonalized wave-number representation of the Fano-Anderson Hamiltonian is given by [30, 56]:

$$H = \sum_{i=0}^{n} \varepsilon_{k_i} c_{k_i}^{\dagger} c_{k_i} + \epsilon b^{\dagger} b + V \sum_{i=0}^{n-1} (c_{k_i}^{\dagger} b + b^{\dagger} c_{k_i}) \delta_{k_i 0}. \tag{4.1}$$

After the Jordan-Wigner transformation Eq. (5.16)becomes (see Appendix 5.1) [56]:

$$\bar{H} = \frac{\epsilon}{2}\sigma_z^1 + \frac{\varepsilon_{k_0}}{2}\sigma_z^2 + \frac{V}{2}(\sigma_x^1\sigma_x^2 + \sigma_y^1\sigma_y^2). \tag{4.2}$$

The drift Hamiltonian in the quantum simulator is:

$$H_{device} = \frac{1}{2}\left(\frac{(\epsilon + \varepsilon_{k_0})}{2} - \sqrt{\left(\frac{\epsilon - \varepsilon_{k_0}}{2}\right)^2 + V^2}\right)\sigma_z^1 + \frac{1}{2}\left(\frac{(\epsilon + \varepsilon_{k_0})}{2} + \sqrt{\left(\frac{\epsilon - \varepsilon_{k_0}}{2}\right)^2 + V^2}\right)\sigma_z^2. \tag{4.3}$$

The authors provide a control sequence to map the Hamiltonian in Eq. (4.2) onto the drift Hamiltonian of Eq. (4.3),

$$U = e^{i\frac{\pi}{4}\sigma_x^2} e^{-i\frac{\pi}{4}\sigma_y^1} e^{-i\frac{\theta}{2}\sigma_z^1\sigma_z^2} e^{i\frac{\pi}{4}\sigma_y^1} e^{i\frac{\pi}{4}\sigma_x^1} e^{-i\frac{\pi}{4}\sigma_x^2} e^{-i\frac{\pi}{4}\sigma_y^2} e^{i\frac{\theta}{2}\sigma_z^1\sigma_z^2} e^{-i\frac{\pi}{4}\sigma_x^1} e^{i\frac{\pi}{4}\sigma_y^2}. \tag{4.4}$$

The final result of this simulation is the time evolution of the state of the impurity. For this purpose the time correlation function $C(t) = b(t)b(0)^{\dagger}$ is calculated. In terms of spin operators: $C(t) = e^{i\bar{H}t}\sigma_-^1 e^{-i\bar{H}t}\sigma_+^1$ [56], where $\sigma_+ = \sigma_x + i\sigma_y$ and $\sigma_- = \sigma_x - i\sigma_y$. The time correlation function provides the overlap of the initial and final states of the impurity.

In this work, we use the Hamiltonian in Eq. (4.2) to perform the unitary evolution of initial states of the system which are not "ideal". We study the final results of the simulation in the presence of errors in the preparation of initial states. Our results also include calculations of the time correlation function, the purpose is to compare the result of this quantum simulation when the initial state is prepared incorrectly or becomes correlated

[t=0] [t=0.3] [t=0.6] [t=0.9]

Figure 4.1. Evolution of the Bloch Vector of the reduced dynamics of qubit 1 in the initial state $\rho_1 = |0\rangle\langle 0|$ as a function of time.

or entangled with other particles in the system, with the result under ideal conditions.

4.1.2 States with Bloch vector in the z direction

We first consider states with only a z component to their Bloch vector. These form a special class of states due to their commutativity of the zz Hamiltonian. Fig. (4.1) is a collection of "snapshots" that represent the evolution of the Bloch vector at different times.

Ideal states and convex combinations of eigenstates of the σ_z operator

The first task is to describe the dynamics of the impurity site when the entire system undergoes closed evolution. The system is composed of the resonant impurity and a fermion it is coupled to, and is not in contact with an external reservoir. However, we are interested only in the dynamics of the impurity (qubit 1), and to obtain the dynamical map for it, it is necessary to perform the partial trace over qubit 2 (the fermion site), and thus look at qubit 1 as the reduced system, and qubit 2 as its environment. We'll eventually look at the dynamics when additional qubits are coupled to the system and are treated as external noise. We first look at two different types of initial states: ideal ones and convex combinations of eigenstates of the σ_z operator. To better identify the maps arising from the reduced dynamics of qubit 1, the initial states are labeled as follows:

A.1 Ideal states: Qubit 1 is in the excited state, qubit 2 is in the ground state.

$$|\psi(0)\rangle = |01\rangle \tag{4.5}$$

Here $|0\rangle$ corresponds to the"spin-up"/occupied state, and $|1\rangle$ is the "spin-down"/unoccupied state. In density operator notation

$$\rho_S(0) = \frac{1}{4}\Big\{ (\mathbb{1} + \sigma_z) \otimes (\mathbb{1} - \sigma_z) \Big\} \tag{4.6}$$

Where the left hand side of the equation is the density operator representing a "spin up" state for qubit one, and the right hand side is the density operator representing a "spin down" state.

A.2 States in a convex combination of states

$$\rho(0) = (1-p)(\rho_1^I \otimes \rho_2^I) + p(\rho_1^{II} \otimes \rho_2^{II}), \tag{4.7}$$

Where p is the probability and the super indexes are used to represent two possible state configurations. The combination was done with varying values of p for:

$$\rho_1^I \otimes \rho_2^I = \frac{1}{4}\,(\mathbb{1} + \sigma_z) \otimes (\mathbb{1} - \sigma_z) \tag{4.8}$$

And

$$\rho_1^{II} \otimes \rho_2^{II} = \frac{1}{4}\,(\mathbb{1} + \sigma_z) \otimes (\mathbb{1} - \sigma_z) \tag{4.9}$$

We used the Bloch vector notation. Each one of the projections along x, y and z will be represented as the arbitrary constants a_1, a_2 and a_3, to obtain a more general result. The class of states in this subsection have $a_1 = 0$, $a_2 = 0$ and $a_3 \neq 0$, i.e. only a component

in the z direction.

Then the initial density operator that represents the state of qubit 1 becomes:

$$\rho_1(0) = \frac{1}{2}\left(\mathbb{1} + a_3\sigma_z\right)$$

The constant a_3 is real and has a numerical value that is equal to or less than the radius of the Bloch sphere ($0 \leq a_3 \leq 1$). And the initial density operator that represents the state of qubit 2 is:

$$\rho_2(0) = \frac{1}{2}\left(\mathbb{1} - \sigma_z\right)$$

The reduced dynamics of ρ_1 after performing the evolution of $\rho_1 \otimes \rho_2$ with the unitary generated by Eq. (4.2) is obtained as follows:

$$\rho_1(t) = \mathrm{Tr}[\rho_S(0)\left(U(t)\rho(0)U(t)^\dagger\right)]$$

Which is a state of the general form:

$$\rho_1(t) = \frac{1}{2}\left(\mathbb{1} + b_3\sigma_z\right)$$

where b_3 is another real constant that is subject to the constraint $0 \leq b_3 \leq 1$. The value of b_3 depends on a_3 and on the parameters ϵ, ε_{k_i}, V and t. The dynamical map A is calculated to act as a direct matrix product on $\rho_1(t)$ in vector form,

$$\begin{pmatrix} 1+b_3 \\ 0 \\ 0 \\ 1-b_3 \end{pmatrix} = A \begin{pmatrix} 1+a_3 \\ 0 \\ 0 \\ 1-a_3 \end{pmatrix} \tag{4.10}$$

The evolution can be described by the following particular form of the A map:

$$A = \begin{pmatrix} \frac{1+b_3}{2} & 0 & 0 & \frac{1+b_3}{2} \\ 0 & 0 & 0 & 0 \\ 0 & 0 & 0 & 0 \\ \frac{1-b_3}{2} & 0 & 0 & \frac{1-b_3}{2} \end{pmatrix}. \tag{4.11}$$

This map is not unique, it is a particular case of the dynamical map that represents the dynamics of the system. It can be seen that there exists some freedom in the terms in the A matrix that are multiplied by the off-diagonal terms in the density operator, this is not explored in the present work though, but is a question for future work.

This A map is not Hermitian, but preserves the hermiticity of ρ_1; it has trace 1 and preserves the trace of ρ_1. Rearrangement of the A map provides the B map:

$$B = \begin{pmatrix} \frac{1+b_3}{2} & 0 & 0 & 0 \\ 0 & \frac{1+b_3}{2} & 0 & 0 \\ 0 & 0 & \frac{1-b_3}{2} & 0 \\ 0 & 0 & 0 & \frac{1-b_3}{2} \end{pmatrix}. \tag{4.12}$$

Which has eigenvalues:

$$\begin{aligned} \lambda_1 &= \frac{1+b_3}{2}, \\ \lambda_2 &= \frac{1+b_3}{2}, \\ \lambda_3 &= \frac{1-b_3}{2}, \\ \lambda_4 &= \frac{1-b_3}{2}, \end{aligned} \tag{4.13}$$

and these are all positive (recall the constraint $b_3 \geq 1$). The eigenvalues of the B map for the ideal state $|01\rangle$ are plotted as a function of time in Figure (4.2), and it is verified that the dynamics of qubit 1, given the ideal initial conditions can be described with a completely positive map.

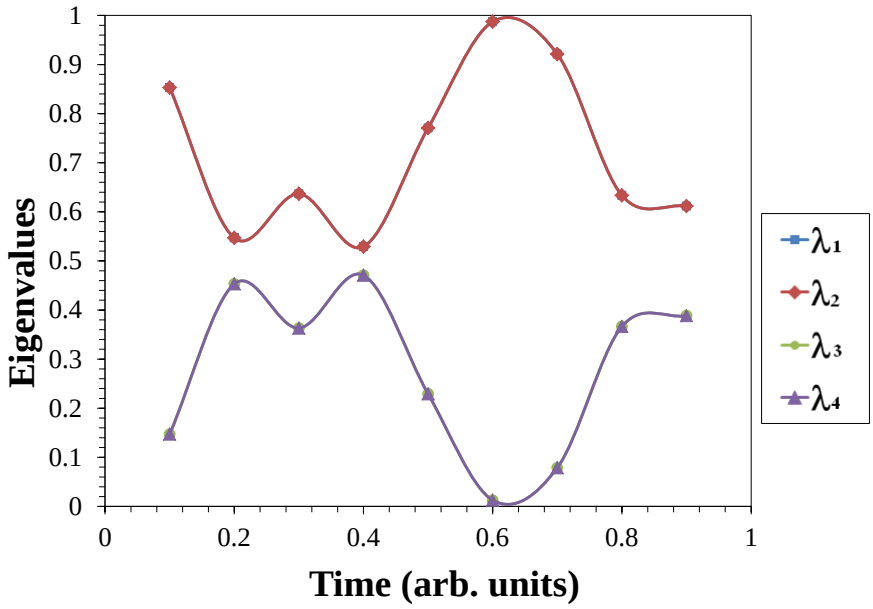

Figure 4.2. Eigenvalues of the dynamical map, B, of the reduced dynamics of qubit 1. The initial state of the *closed* system is $|\psi\rangle = |01\rangle$. This is an example of an ideal state (case $A.1$) with zero quantum discord. The parameters of the Hamiltonian are $\epsilon = -8$ meV, $\varepsilon = -2$ meV, $V = 4$ meV. The evolution was carried out for the time interval $\Delta t \in [0.1, 0.9]$. There are four sets of eigenvalues, but due to form of the dynamical map two of these sets appear to overlap with the other two sets, which is the reason why only two lines show on the graph.

We found that a similar map is obtained for initial states in a convex combination of the form in (A.2), but this is the case only when the individual states of the particles have only z components to their Bloch vector.

Ideal states and convex combinations eigenstates of the σ_z operator with noise

To add external noise to the system, we included environmental qubits that interact with the system. We did so by modifying the control Hamiltonian. In this context, we examine two different models of noise:

1. First, we added two spins and had them interacting via zz coupling with the particle that represents the state of the fermion site (see Fig. (4.3)):

$$\begin{aligned} H_{\text{NMR}} &= \frac{1}{2}\left(\frac{(\epsilon+\varepsilon_{k_0})}{2}-\sqrt{\left(\frac{\epsilon-\varepsilon_{k_0})}{2}\right)^2+V^2}\right)\sigma_z^1 \\ &+\frac{1}{2}\left(\frac{(\epsilon+\varepsilon_{k_0})}{2}+\sqrt{\left(\frac{(\epsilon-\varepsilon_{k_0})}{2}\right)^2+V^2}\right)\sigma_z^2 \\ &+\frac{J_{zz}}{4}\sigma_z^2\sigma_z^3+\frac{J_{zz}}{4}\sigma_z^2\sigma_z^4+\frac{J_{zz}}{4}\sigma_z^3\sigma_z^4. \end{aligned} \tag{4.14}$$

2. Next, we added an extra particle, which interacts in the same fashion (zz coupling) with both particles that represent the system of interest: the resonant impurity and the fermion site (see Fig. (4.4)):

$$\begin{aligned} H_{NMR} &= \frac{1}{2}\left(\frac{(\epsilon+\varepsilon_{k_0})}{2}-\sqrt{\left(\frac{\epsilon-\varepsilon_{k_0})}{2}\right)^2+V^2}\right)\sigma_z^1 \\ &+\frac{1}{2}\left(\frac{(\epsilon+\varepsilon_{k_0})}{2}+\sqrt{\left(\frac{(\epsilon-\varepsilon_{k_0})}{2}\right)^2+V^2}\right)\sigma_z^2 \\ &+\frac{J_{zz}}{4}\sigma_z^1\sigma_z^3+\frac{J_{zz}}{4}\sigma_z^2\sigma_z^3, \end{aligned} \tag{4.15}$$

where J_{zz} represents the zz coupling constant. To simulate an experiment, we performed the same control sequence in Eq. (4.4) to obtain Eq. (4.2). By doing this we assume the experimentalist is not aware of the presence of unwanted interactions with external qubits and will find out the effects of the errors in the outcome of the simulation.

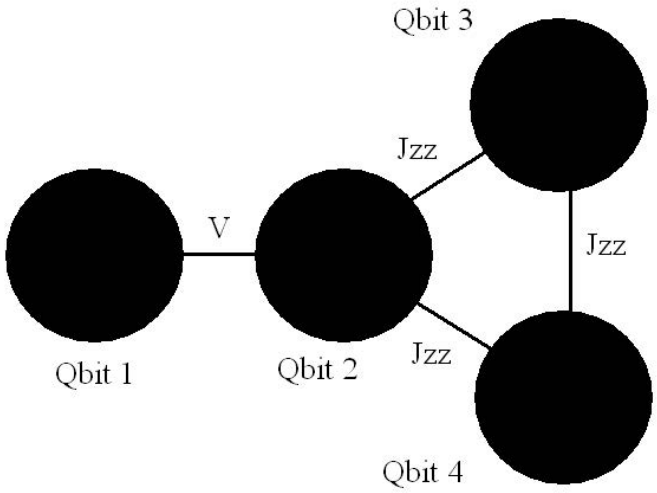

Figure 4.3. Schematic representation of the simulated system. qubit 1 is used to simulate the resonant impurity and qubit 2 represents a fermion site. The two particles interact via the potential V. qubit 2 interacts with two external spins (qubits 3 and 4) through the coupling term J_{zz}.

In this section we present the results for systems governed by the Hamiltonians in Eqs. (4.14) and (4.15). The initial state of the bath must be specified in the initial state of the system. We also chose different initial configurations of the state of qubits 1 and 2 in order to observe the effects of noise with errors in the preparation. These are:

A.3 Ideal states

$$|\psi(0)\rangle = |0111\rangle \tag{4.16}$$

and the density operator can be obtained from the outer product $\rho(0) = |\psi(0)\rangle \langle\psi(0)|$, or calculated as the tensor product of the density operators representing the states of all the qubits. For states that only have a z component in the Bloch vector, these density matrices can be written in the same form as those of case A.1.

A.4 Convex combinations of eigenstates of the σ_z operator, which are an extension of case

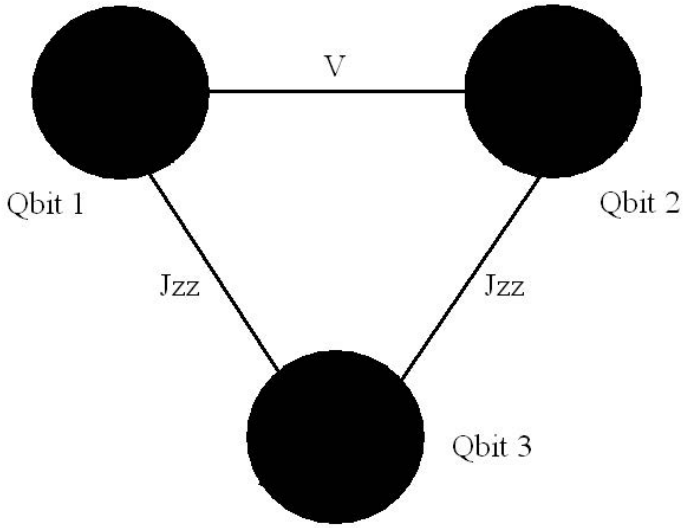

Figure 4.4. Schematic representation of the simulated system. qubit 1 is used to simulate the resonant impurity and qubit 2 represents a fermion site. The two particles interact via the potential V, and with an external spin (qubit 3) through the coupling term J_{zz}.

A.2, but one or both qubits in the system interact with external ones:

$$\rho(0) = \left((1-p)(\rho_1^I \otimes \rho_2^I) + p(\rho_1^{II} \otimes \rho_2^{II})\right) \otimes (|1\rangle\langle 1|) \otimes (|1\rangle\langle 1|) \tag{4.17}$$

. The states of the bath qubits are in the same basis as those in the system, to study the simplest scenario.

The initial state of qubit 1 can be written as an arbitrary Bloch vector of the form:

$$\rho_S(0) = \mathrm{Tr}_E \rho(0) = \frac{1}{2}(\mathbb{1} + a_3\sigma_z). \tag{4.18}$$

And the reduced dynamics of qubit 1 after time t is:

$$\rho_1(t) = \mathrm{Tr}_E\left(U(t)\rho(0)U(t)^\dagger\right) = \frac{1}{2}(\mathbb{1} + b_3\sigma_z), \tag{4.19}$$

a_3 and b_3 are arbitrary constants with numerical value which is less than or equal to the value of the radius of the Bloch sphere. Then, once again, the A map is obtained to satisfy

$$\begin{pmatrix} 1+b_3 \\ 0 \\ 0 \\ 1-b_3 \end{pmatrix} = A \begin{pmatrix} 1+a_3 \\ 0 \\ 0 \\ 1-a_3 \end{pmatrix} \tag{4.20}$$

And because the evolution only causes variations in the magnitude of the z component in the Bloch vector, the A map is similar to that in Eq. (4.11):

$$A = \begin{pmatrix} \frac{1+b_3}{2} & 0 & 0 & \frac{1+b_3}{2} \\ 0 & 0 & 0 & 0 \\ 0 & 0 & 0 & 0 \\ \frac{1-b_3}{2} & 0 & 0 & \frac{1-b_3}{2} \end{pmatrix}. \tag{4.21}$$

From which the B map is obtained, and is similar to Eq. (4.12),

$$B = \begin{pmatrix} \frac{1+b_3}{2} & 0 & 0 & 0 \\ 0 & \frac{1+b_3}{2} & 0 & 0 \\ 0 & 0 & \frac{1-b_3}{2} & 0 \\ 0 & 0 & 0 & \frac{1-b_3}{2} \end{pmatrix}. \tag{4.22}$$

The purpose of adding noise is to observe the effects on the final result of the simulation, but also on the reduced dynamics. Because this is a simple case in which there is only a zz coupling, we found that the strength of J_{zz} affects only the rate of change of

the state of qubit 1, which is more evident in the time correlation function, but has no effect on the complete positivity of the dynamical map. This can be seen in Figs. (4.6) and (4.7), where the eigenvalues of B are plotted with the couplings to the particles of the spin bath being $J_{zz} = 8$ and $J_{zz} = \frac{1}{10}$ respectively.

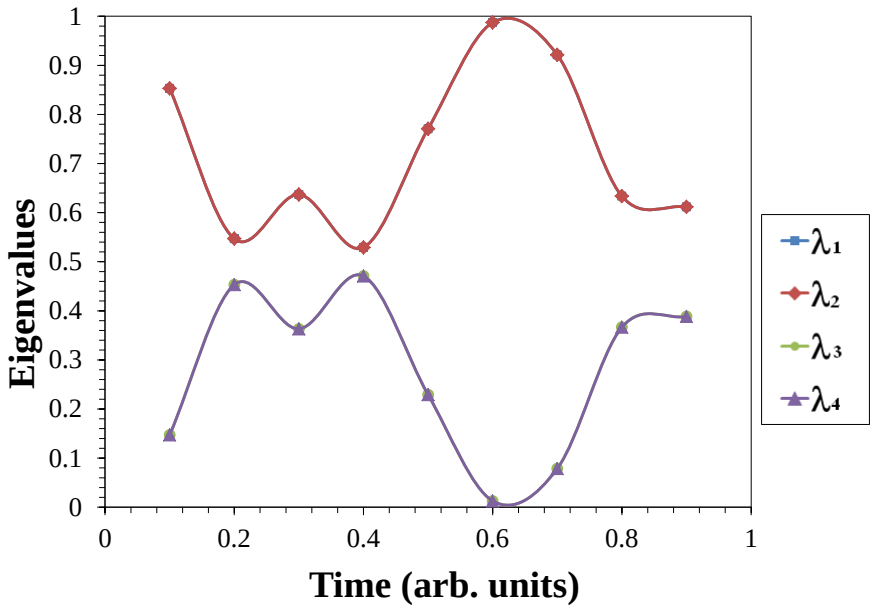

Figure 4.5. Eigenvalues of the dynamical map, B, of the reduced dynamics of qubit 1. The initial state of the *closed* system is $|\psi\rangle = |01\rangle$. This is an example of an initially ideal state (case $A.1$) with zero quantum discord. The parameters of the Hamiltonian are $\epsilon = -8$ meV, $\varepsilon = -2$ meV, $V = 4$ meV. The evolution was carried out for the time interval $\Delta t \in [0.1, 0.9]$. There are four sets of eigenvalues, but due to form of the dynamical map two of these sets appear to overlap with the other two sets, which is the reason why only two lines show on the graph.

Figs. (4.2), (4.6) and (4.7) show the evolution of the same initial state but each has a different environment. The class of states that had only a z component to their Bloch vector correspond to completely positive reduced dynamics, since the interaction with the bath is only through zz coupling. However, it does change the hopping rate and is visible

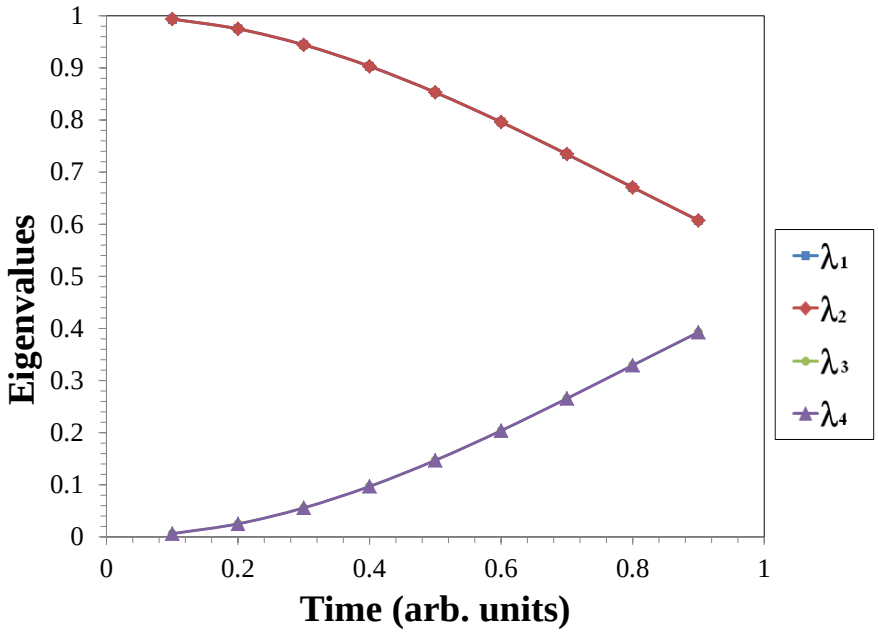

Figure 4.6. Eigenvalues of the dynamical map of the reduced dynamics of qubit 1. In the open system two qubits are interacting via zz coupling with qubit 2 with coupling constant $J_{zz} = 8$ meV. The initial state of the system and bath is given by $\psi = |0111\rangle$ (case A.3). The system parameters are $\epsilon = -8$ meV, $\varepsilon = -2$ meV and $V = 4$ meV. The evolution is carried out for the time interval $t \in [0.1, 0.9]$. The dynamical map of the reduced dynamics for this configuration is also completely positive. Similarly to the case of Fig. (4.2), there are two sets of eigenvalues which overlap, and the type of coupling to the bath qubits affects the rate of change, but not the complete positivity of the reduced dynamics.

in the time correlation function, which will be discussed in the next sections. In Fig. (4.6) the effect on the rate of change is particularly noticeable due to the choice of the coupling. The state of the impurity does not transfer as quickly due to the strong correlations generated by the interaction with the spin bath. In Fig. (4.7) the situation is different. In this case the eigenvalues remained the same regardless of the strength of the coupling with the environment.

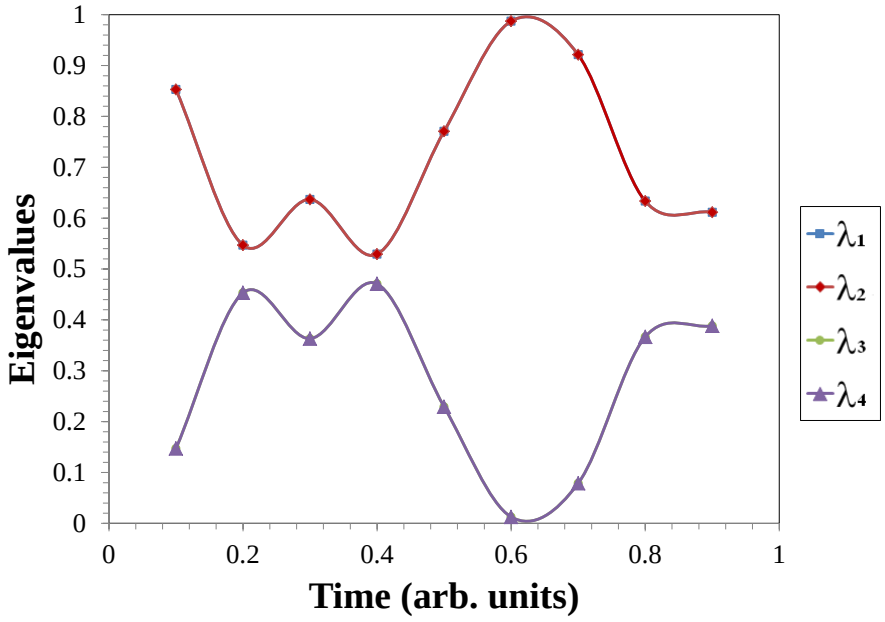

Figure 4.7. Eigenvalues of the dynamical map of the reduced dynamics of qubit 1. The system is open. An additional qubit is interacting via zz coupling with qubits 1 and 2 with coupling constant $J_{zz} = 1/10$ meV. The initial state of the system and bath is $|\psi\rangle = |011\rangle$ (case A.4 with only one additional qubit). The system parameters are $\epsilon = -8$ meV, $\varepsilon = -2$ meV and $V = 4$ meV. The evolution is carried out for the time interval $t \in [0.1, 0.9]$. This configuration was the same as in Fig. (4.2) because the couplings to the third qubit both had the same magnitude, which results in a shift in the values of the energies, but the relative sizes of the parameters remain unchanged.

4.1.3 States with an x component to their Bloch vector

To represent an error in the preparation of a quantum state, we chose to add an x component to the polarization vector that represents the initial state of qubit 1. In this section we consider an initial state with a component of the Bloch vector in the x direction. A visual representation of a state of this kind can be seen in Fig. (4.8). Clearly a y component is not necessary, and only specifies a different initial condition for the angle

since the system will precess.

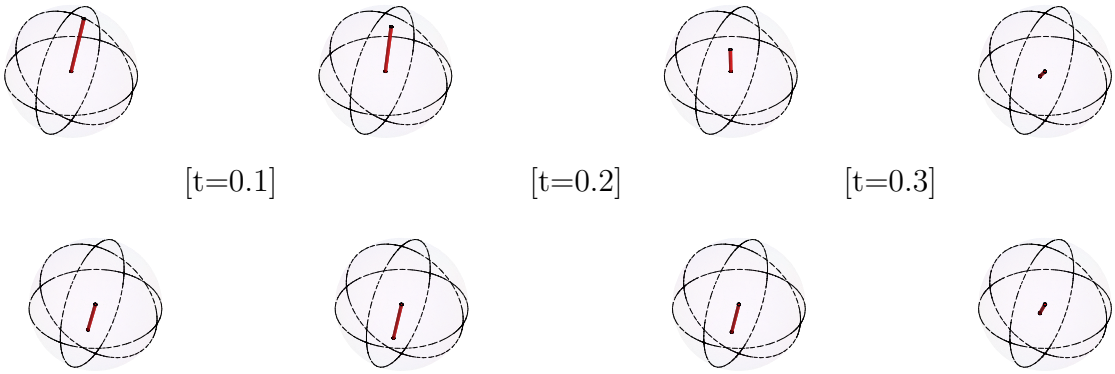

Figure 4.8. Animation of the evolution of the Bloch Vector of the reduced dynamics of qubit 1 in the initial state $\rho_1 = \frac{1}{2}(\mathbb{1} + 0.2\sigma_x + 0.97\sigma_z)$

Closed system evolution

The initial states were chosen to have a component in the x direction; the components in x and z were selected such that the magnitude of the Bloch vector is close or equal to 1 emulating a small error in the initialization. The initial state configurations are:

B.1 States in which qubit 1 has a component in the x direction

$$\rho_1(0) = \frac{1}{2}(\mathbb{1} + a_1\sigma_x + a_3\sigma_z)$$

and

$$\rho_2(0) = \frac{1}{2}(\mathbb{1} - \alpha_3\sigma_z)$$

B.2 A convex combination of states; one (or both) of the possible states of qubit 1 has a

component in the x direction (state for qubit 1 in case B.1)

$$\rho(0) = \left((1-p)(\rho_1^I \otimes \rho_2^I) + p(\rho_1^{II} \otimes \rho_2^{II})\right),$$

Where ρ_1 is the state of the impurity, ρ_2 is the state of the fermion and the a_i are subject to $0 \leq \sqrt{a_1^2 + a_3^2} \leq 1$.

After performing a "global" unitary evolution of the system, we take the partial trace over qubit 2, which results in the final state of qubit 1, and for this class of states, we obtained a state of the form:

$$\rho_1(t) = \mathrm{Tr}_E\left(U\rho(0)U^\dagger\right) = \frac{1}{2}(\mathbb{1} + b_1\sigma_x + b_2\sigma_y + b_3\sigma_z) \tag{4.23}$$

Because the final state has components in x, y and z, a particular A map that satisfies:

$$\begin{pmatrix} 1+b_3 \\ b_1 - ib_2 \\ b_1 + ib_2 \\ 1-b_3 \end{pmatrix} = A \begin{pmatrix} 1+a_3 \\ a_1 \\ a_1 \\ 1-a_3 \end{pmatrix} \tag{4.24}$$

Is given by

$$A = \begin{pmatrix} \frac{1+b_3}{2} & 0 & 0 & \frac{1+b_3}{2} \\ 0 & \frac{-ib_2}{a_1} & \frac{b_1}{a_1} & 0 \\ 0 & \frac{b_1}{a_1} & \frac{ib_2}{a_1} & 0 \\ \frac{1-b_3}{2} & 0 & 0 & \frac{1-b_3}{2} \end{pmatrix} \tag{4.25}$$

Analytically, the b_i parameters can be evaluated by performing the partial trace using arbitrary initial parameters a_i for the state of qubit 1, and arbitrary parameters of the system:

$$b_i = \mathrm{Tr}\rho(t)(\sigma_i \otimes \mathbb{1}) \tag{4.26}$$

Where $\rho(t)$ is the final state of the system. The σ_i are the Pauli spin matrix operators for $i = x, y, z$. The analytical expression for the b_i parameters becomes

$$\begin{aligned} b_1 = \Bigg\{ &\cos\left(\frac{1}{2}t(\epsilon+\varepsilon_{k_0})\right)\cos\left(\frac{1}{2}t\sqrt{4V^2+(\epsilon-\varepsilon_{k_0})^2}\right) \\ &-\sin\left(\frac{1}{2}t(\epsilon+\varepsilon_{k_0})\right)\left[\frac{(\epsilon-\varepsilon)\sin\left(\frac{1}{2}t\sqrt{4V^2+(\epsilon-\varepsilon_{k_0})^2}\right)}{\sqrt{4V^2+(\epsilon-\varepsilon_{k_0})^2}}\right]\Bigg\}a_1, \end{aligned} \tag{4.27}$$

$$\begin{aligned} b_2 = \Bigg\{ &-\sin\left(\frac{1}{2}t(\epsilon+\varepsilon_{k_0})\right)\cos\left(\frac{1}{2}t\sqrt{4V^2+(\epsilon-\varepsilon_{k_0})^2}\right) \\ &-\cos\left(\frac{1}{2}t(\epsilon+\varepsilon_{k_0})\right)\left[\frac{(\epsilon-\varepsilon)\sin\left(\frac{1}{2}t\sqrt{4V^2+(\epsilon-\varepsilon_{k_0})^2}\right)}{\sqrt{4V^2+(\epsilon-\varepsilon_{k_0})^2}}\right]\Bigg\}a_1 \end{aligned}$$

and

(4.28)

$$b_3 = \frac{2(-1+a_3)V^2 + a_3(\epsilon-\varepsilon)^2 + (1+a_3)V^2\cos\left(t\sqrt{4V^2+(\epsilon-\varepsilon)^2}\right)}{4V^2+(\epsilon-\varepsilon)^2}. \tag{4.29}$$

And A can be rewritten,

$$A = \begin{pmatrix} \frac{1+b_3}{2} & 0 & 0 & \frac{1+b_3}{2} \\ 0 & -ic_2 & c_1 & 0 \\ 0 & c_1 & ic_2 & 0 \\ \frac{1-b_3}{2} & 0 & 0 & \frac{1-b_3}{2} \end{pmatrix} \tag{4.30}$$

The A map is then found to be linear (independent of the initial state), and then the B map can be obtained:

$$B = \begin{pmatrix} \frac{1+b_3}{2} & 0 & 0 & -ic_2 \\ 0 & \frac{1+b_3}{2} & c_1 & 0 \\ 0 & c_1 & \frac{1-b_3}{2} & 0 \\ ic_2 & 0 & 0 & \frac{1-b_3}{2} \end{pmatrix} \tag{4.31}$$

The eigenvalues of B are given by

$$\begin{aligned} \lambda_1 &= \frac{1-\sqrt{4c_1^2+b_3^2}}{2} \qquad & \lambda_2 &= \frac{1+\sqrt{4c_1^2+b_3^2}}{2} \\ \lambda_3 &= \frac{1-\sqrt{4c_2^2+b_3^2}}{2} \qquad & \lambda_4 &= \frac{1+\sqrt{4c_2^2+b_3^2}}{2} \end{aligned} \tag{4.32}$$

The plot of these eigenvalues as a function of time in Figure (4.9) shows that this is a non completely positive map: For a state of the form B.2, it can be found that a similar dynamical map describes the reduced dynamics. The shape of the graph changes with the variation of the parameter p (the probability of being in one state or the other for states of the form B.2), but its found to be mostly NCP for this system and the selected set of parameters. Nevertheless, the dynamical map preserves the properties of the density operator representing the quantum mechanical state of qubit 1.

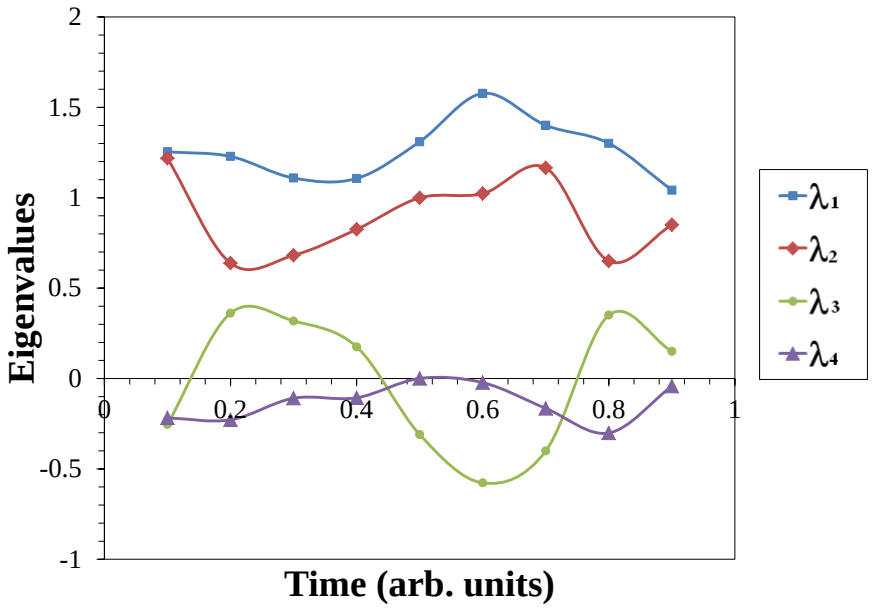

Figure 4.9. Eigenvalues of the dynamical map of the reduced dynamics of qubit 1. The initial states of the qubits in the closed system are $\rho_1 = \frac{1}{2}(\mathbb{1} + 0.2\sigma_x + 0.97\sigma_z)$ and $\rho_2 = \frac{1}{2}(\mathbb{1} - \sigma_z)$ (case B.1). The parameters of the Hamiltonian are $\epsilon = -8$ meV, $\varepsilon = -2$ meV, $V = 4$ meV. The evolution is carried out for the time interval $t \in [0.1, 0.9]$.

We want to recall the composition of maps. As mentioned in Chapter 2, there are three maps that compose the total dynamical map B: the assignment map, the unitary map and the trace over the environment. The unitary and the trace must be completely positive, it is the assignment map, the one that puts a state in the space of S (the system, but in this particular case it is in the space of qubit 1) to a state in the space SE (the space system plus environment, in this case, our total system, the space of qubits 1 and 2), where we should look for the conditions for complete or not complete positivity. As mentioned in chapter (2), the assignment map must satisfy the following conditions:

1. It is linear

2. It is consistent

3. It is completely positive

According to [28, 115], giving up consistency can result in a loss of linearity, and therefore it is preferable to give up complete positivity of the assignment map. In this particular case, we can think of the error in the initial state. If the system is prepared in the state $|01\rangle$, but an error in the state results in an initial state of the form B.1, then the dynamics cannot be described by the CP map in Eq. (4.12), because the final state of the form of the final state. This can be thought of as an giving up consistency, but can also be thought of giving up complete positivity. But in both cases linearity is preserved.

Open system evolution

The results in this subsection are generated from adding the qbits in the spin bath, and using the following initial states

B.3 States in which qubit 1 has a component in the x direction in an open system

$$\rho(0) = \rho_1(0) \otimes \rho_2(0) \otimes (|1\rangle \langle 1|) \otimes (|1\rangle \langle 1|), \tag{4.33}$$

where

$$\rho_1(0) = \frac{1}{2}(\mathbb{1} + a_1\sigma_x + a_3\sigma_z), \tag{4.34}$$

and

$$\rho_2(0) = \frac{1}{2}(\mathbb{1} - \alpha_3\sigma_z). \tag{4.35}$$

The reduced dynamics of S are given by

$$\rho(t) = \mathrm{Tr}_E\left(U(t)\rho(0)U(t)^\dagger\right) = \frac{1}{2}(\mathbb{1} + b_1\sigma_x + b_2\sigma_y + b_3\sigma_z), \tag{4.36}$$

with a B map of the same for as that in Eq. (4.31),

$$B = \begin{pmatrix} \frac{1+b_3}{2} & 0 & 0 & -ic_2 \\ 0 & \frac{1+b_3}{2} & c_1 & 0 \\ 0 & c_1 & \frac{1-b_3}{2} & 0 \\ ic_2 & 0 & 0 & \frac{1-b_3}{2} \end{pmatrix}. \tag{4.37}$$

The coupling strength to the bath qubits has an effect on the time correlation function, but not necessarily on the positivity or not complete positivity of the dynamical map. This can be seen in Figs. (4.10) and (4.11), where the eigenvalues of the B map are calculated as functions of time.

Dynamical maps obtained through quantum process tomography can present discrepancies if the initial states are prepared through different experimental methods [89]. Thus the off diagonal term due to the x component can represent an error, which gives rise to a NCP map like in the previous case. Note that Fig. (4.11) is very similar to Fig. (4.9). In Fig. (4.11) the two qubits in the system are interacting with an external spin. Because this interaction is due to a zz coupling to the bath of the same strength for both particles, it represents only a shift in the parameters of the system. Therefore, the dynamics are the same in both cases. However, in Fig. (4.10) only qubit 2 is interacting with two external spins, and there is an effect on the shape of the eigenvalues plot, but not on the positivity or complete positivity. The rate of change of the system changes when there are effects of noise in the Hamiltonian, this can be verified with the time correlation function which will be discussed in the next sections.

4.1.4 Completely or not completely positive dynamics?

Before proceeding to observing the effects of either the correlations in the initial state, or the coupling to the bath on the final time correlation function, we will analyze the

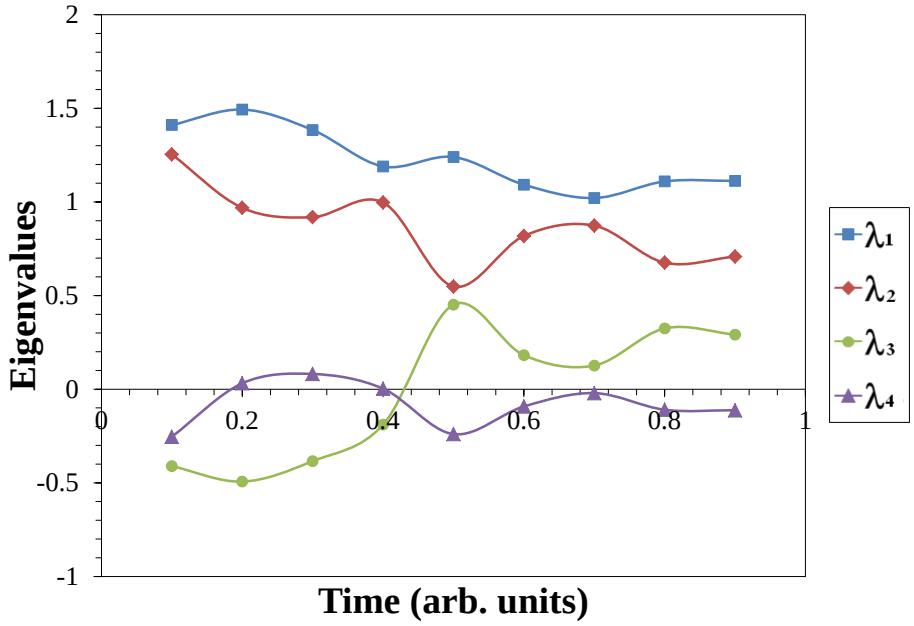

Figure 4.10. Eigenvalues of the dynamical map for the reduced dynamics of qubit 1. The initial states of the particles in the system are $\rho_1 = \frac{1}{2}(\mathbb{1} + 0.2\sigma_x + 0.97\sigma_z)$ and $\rho_2 = \frac{1}{2}(\mathbb{1} - \sigma_z)$. The initial states of the particles that compose the spin bath are $\rho_3 = \frac{1}{2}(\mathbb{1} - \sigma_z)$ and $\rho_4 = \frac{1}{2}(\mathbb{1} - \sigma_z)$. The total state of the bath is an example of case B.3. The Hamiltonian parameters are $\epsilon = -8$ meV, $\varepsilon = -2$ meV, $V = 4$ meV. The coupling to the bath has strength $J_{zz} = 6$ meV. The evolution is carried out in the time interval $t \in [0.1, 0.9]$.

dynamical maps that describe the non- completely positive evolution. For the state that presented an error in the preparation, we had that qubit 1 was initially of the form

$$\rho_1(0) = \frac{1}{2}(\mathbb{1} + a_1\sigma_x + a_3\sigma_z) \tag{4.38}$$

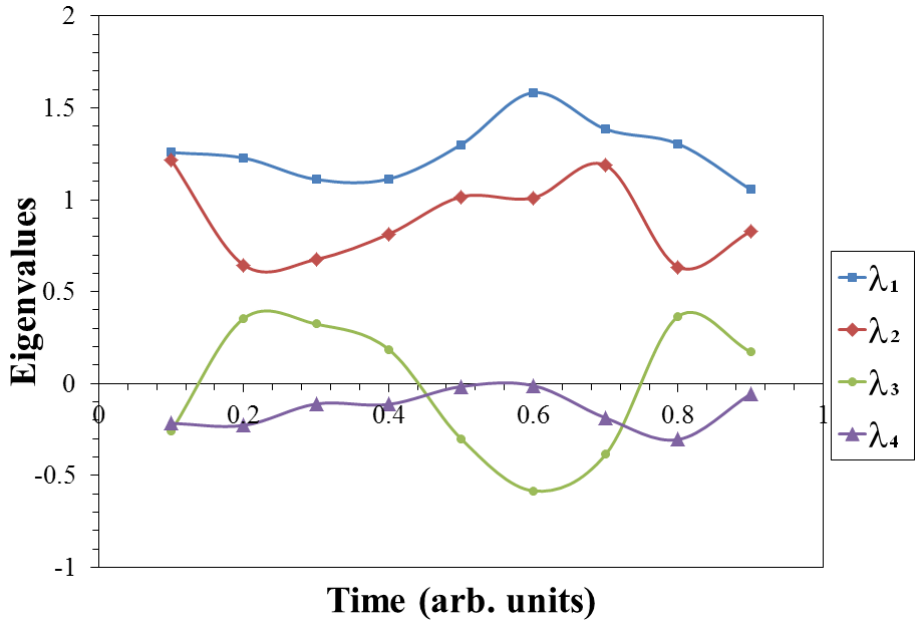

Figure 4.11. Eigenvalues of the dynamical map for the reduced dynamics of qubit 1. The initial states of the particles in the system are $\rho_1 = \frac{1}{2}(\mathbb{1} + 0.2\sigma_x + 0.97\sigma_z)$ and $\rho_2 = \frac{1}{2}(\mathbb{1} - \sigma_z)$. The initial state of the additional qubit is $\rho_3 = \frac{1}{2}(\mathbb{1} - \sigma_z)$. This is another form of case B.3, except that there is only one additional qubit acting as the bath. The Hamiltonian parameters are $\epsilon = -8$ meV, $\varepsilon = -2$ meV, $V = 4$ meV. The coupling to the additional qubit has strength $J_{zz} = \frac{1}{10}$ meV. The evolution of the system is evaluated for the time interval $t \in [0.1, 0.9]$.

Then the direct multiplication matrix was give by

$$A = \begin{pmatrix} \frac{1+b_3}{2} & 0 & 0 & \frac{1+b_3}{2} \\ 0 & -ic_2 & c_1 & 0 \\ 0 & c_1 & ic_2 & 0 \\ \frac{1-b_3}{2} & 0 & 0 & \frac{1-b_3}{2} \end{pmatrix} \tag{4.39}$$

And that recasts onto the B map:

$$B = \begin{pmatrix} \frac{1+b_3}{2} & 0 & 0 & -ic_2 \\ 0 & \frac{1+b_3}{2} & c_1 & 0 \\ 0 & c_1 & \frac{1-b_3}{2} & 0 \\ ic_2 & 0 & 0 & \frac{1-b_3}{2} \end{pmatrix}. \tag{4.40}$$

Whose action on $\rho_1(0)$ is defined as follows:

$$\rho(t) = B\left[\rho(0)\right] = \sum_{\alpha} \lambda_\alpha \zeta_\alpha \rho(0) \zeta_\alpha^\dagger, \tag{4.41}$$

Where λ_α and ζ_α are the eigenvalues and eigenmatrices of B, respectively. There exists an alternative map, which is completely positive The direct matrix product is

$$A^{'} = \begin{pmatrix} \frac{1+b_3}{2} & 0 & 0 & \frac{-ib_2}{a_1} \\ \frac{b_1-ib_2}{2} & 0 & 0 & \frac{b_1-ib_2}{2} \\ \frac{b_1+ib_2}{2} & 0 & 0 & \frac{b_1+ib_2}{2} \\ \frac{1-b_3}{2} & 0 & 0 & \frac{1-b_3}{2} \end{pmatrix}. \tag{4.42}$$

Which becomes the $B^{'}$ map

$$B^{'} = \begin{pmatrix} \frac{1+b_3}{2} & 0 & \frac{b_1-ib_2}{2} & 0 \\ 0 & \frac{1+b_3}{2} & 0 & \frac{b_1-ib_2}{2} \\ \frac{b_1+ib_2}{2} & 0 & \frac{1-b_3}{2} & 0 \\ 0 & \frac{b_1+ib_2}{2} & 0 & \frac{1-b_3}{2} \end{pmatrix} \tag{4.43}$$

The $B^{'}$ map is Hermitian, trace 2 and has eigenvalues:

$$\lambda_1 = \frac{1-\sqrt{b_1^2+b_2^2+b_3^2}}{2}, \qquad \lambda_2 = \frac{1-\sqrt{b_1^2+b_2^2+b_3^2}}{2},$$
$$\lambda_3 = \frac{1+\sqrt{b_1^2+b_2^2+b_3^2}}{2}, \qquad \lambda_4 = \frac{1+\sqrt{b_1^2+b_2^2+b_3^2}}{2}, \tag{4.44}$$

Which are all positive, given the restriction $\sqrt{b_1^2+b_2^2+b_3^2} \leq 1$. These maps preserve the Hermiticity, positivity and trace of $\rho_1(t)$, so the question is why use an NCP map? why is the B map in Eq. (4.40) more adequate to describe the reduced dynamics of ρ_1?

To answer this question, we will look at a particular example, of the reduced dynamics of qubit 1, given the parameters $\epsilon = -8$ meV, $\varepsilon = -2$ meV, $V = 4$ meV and $t = 0.9$ arb. units. The initial state of qubit 1 is then given by:

$$\rho_1(0) = \frac{1}{2}\left(\mathbb{1} + 0.2\sigma_x + 0.97\sigma_z\right) \tag{4.45}$$

The initial state of qubit 2 is given by

$$\rho_2(0) = \frac{1}{2}\left(\mathbb{1} - \sigma_z\right) \tag{4.46}$$

Then the evolution of $\rho_S(0) = \rho_1(0) \otimes \rho_2(0)$ is carried out with the unitary:

$$\exp -i\left(\frac{\epsilon}{2}\sigma_z^1 + \frac{\varepsilon_{k_0}}{2}\sigma_z^2 + \frac{V}{2}(\sigma_x^1\sigma_x^2 + \sigma_y^1\sigma_y^2)\right)t \tag{4.47}$$

The reduced dynamics of qubit 1 are then,

$$\rho_1(0) = \frac{1}{2}\left(\mathbb{1} - 0.105781\sigma_x - 0.65939\sigma_y + 0.988347\sigma_z\right) \tag{4.48}$$

The operator-sum decomposition of Eq. (4.40) is given by the following eigenvalues:

$$\lambda_1 = \frac{1-\sqrt{4c_1^2+b_3^2}}{2}, \qquad \lambda_2 = \frac{1+\sqrt{4c_1^2+b_3^2}}{2},$$
$$\lambda_3 = \frac{1-\sqrt{4c_2^2+b_3^2}}{2}, \qquad \lambda_4 = \frac{1+\sqrt{4c_2^2+b_3^2}}{2}, \tag{4.49}$$

And the eigenmatrices

$$\begin{pmatrix} 0 & \frac{b_3-\sqrt{4c_1^2+b_3^2}}{2c_1} \\ 1 & 0 \end{pmatrix}$$

$$\begin{pmatrix} 0 & \frac{b_3+\sqrt{4c_1^2+b_3^2}}{2c_1} \\ 1 & 0 \end{pmatrix}$$

$$\begin{pmatrix} i\frac{-b_3+\sqrt{4c_1^2+b_3^2}}{2c_1} & 0 \\ 0 & 1 \end{pmatrix}$$

$$\begin{pmatrix} i\frac{-b_3-\sqrt{4c_1^2+b_3^2}}{2c_1} & 0 \\ 0 & 1 \end{pmatrix}$$

Which, when acting on $\rho_1(0)$, the final state is given by:

$$\begin{pmatrix} 0.994173 & -0.0528904 + i0.0329695 \\ -0.0528904 - i0.0329695 & 0.00582657 \end{pmatrix}$$

Which is numerically exactly as Eq. (4.48). Now, lets look at the action of $B^{'}$; the eigenmatrices of Eq. (4.43) are:

$$\begin{pmatrix} 0 & \frac{b_3 - \sqrt{b_1^2+b_1^2+b_3^2}}{b_1+ib_2} \\ 0 & 1 \end{pmatrix}$$

$$\begin{pmatrix} \frac{b_3 - \sqrt{b_1^2+b_1^2+b_3^2}}{b_1+ib_2} & 0 \\ 1 & 0 \end{pmatrix}$$

$$\begin{pmatrix} 0 & \frac{b_3 + \sqrt{b_1^2+b_1^2+b_3^2}}{b_1+ib_2} \\ 0 & 1 \end{pmatrix}$$

$$\begin{pmatrix} \frac{b_3 + \sqrt{b_1^2+b_1^2+b_3^2}}{b_1+ib_2} & 0 \\ 1 & 0 \end{pmatrix}$$

The action of the $B^{'}$ map in Eq. (4.43) results in the final state

$$\begin{pmatrix} 0.984146 & -0.053566 + i0.0326367 \\ -0.053566 - i0.0326367 & 0.00577408 \end{pmatrix}$$

Which numerically, is not exactly the same as Eq. (4.48), the way Eq. (4.50) is.

In this particular system, the reduced dynamics of qubit 1 are better described by a map of the form of that in Eq. (4.40), which is NCP. The restriction of complete positivity may exclude many physical situations, because even when we found a CP map, the dynamics are close numerically, but not exact.

4.1.5 Time correlation function

Ortiz et al. calculated the time correlation function $C(t) = b(t)b(0)^{\dagger}$, and plotted the result as $|G|^2 = \mathrm{Tr}\,(\rho(t)\rho(0))$ as a function of time. One of the purposes is to observe the effect of errors in the preparation of initial states in quantum simulations. The numerical results are summarized in graphs, Figs. (4.12), (4.15) and (4.13).

Errors due to state preparation

In Fig. (4.12), there is a slight difference between the results of the original system compared to those under which errors could arise due to noise and unknown initial states. The coupling to the environment affects how fast or slow qubit 1 evolves. However, if the coupling to the bath is weak, these errors are not as visible.

When the initial state had a small component in x, the resulting correlation functions were very close to the original problem. The deviation may increase if there is a smaller z component, making its detection easier. An error like this one, which represents an error in the preparation of an initial state, may not be easily identified at the end of the simulation. Errors of this type are interesting in the context of open quantum system dynamics and

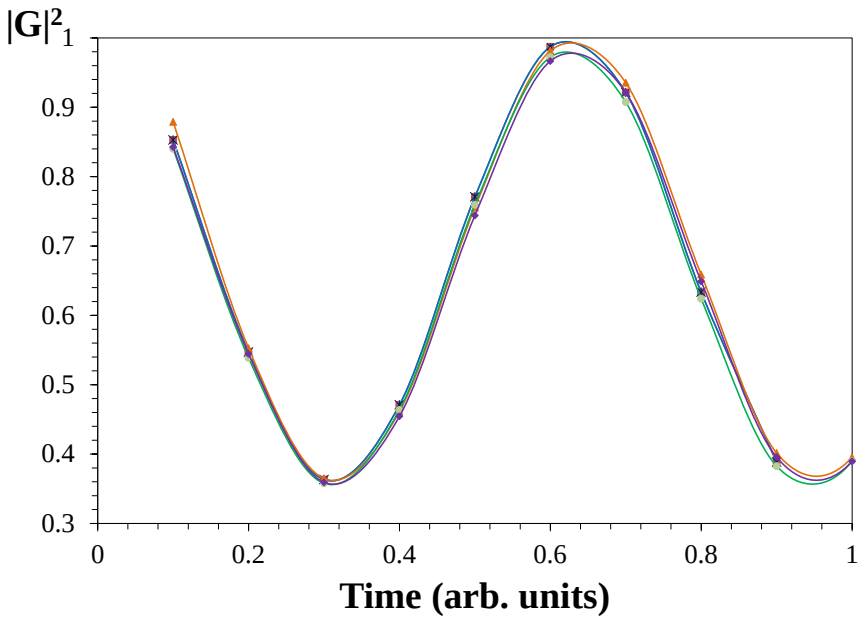

Figure 4.12. Time correlation function of the reduced dynamics of qubit 1. The Hamiltonian parameters are $\epsilon = -8$ meV, $\varepsilon = -2$ meV, $V = 4$ meV. $t \in [0.1, 1]$. These results represent the evolution of the closed system, the system where qubit 2 interacts with two additional qubits, the system in which an additional qubit that interacts with qbits 1 and 2. This was done when qubit 1 was in the initial states $\rho = |0\rangle\langle 0|$ and $\rho = \frac{1}{2}(\mathbb{1} + 0.2\sigma_x + 0.97\sigma_z)$, as indicated above.

the consistency, complete positivity or both, of the assignment map.

In Fig. (4.13), we increased a_1, the component of the Bloch vector in x, to see how it affects the final result. When the x component of the Bloch vector is increased, we can see shifts in the time correlation function from its original position. The smaller a_3 is, the larger the observed shift. Thus, a small error of this type may not be easily detected.

In Figure (4.14) we plot the time correlation function for different initial states. Errors in the form of small x components in the Bloch vector are not very visible, but convex combinations show a more significant deviation.

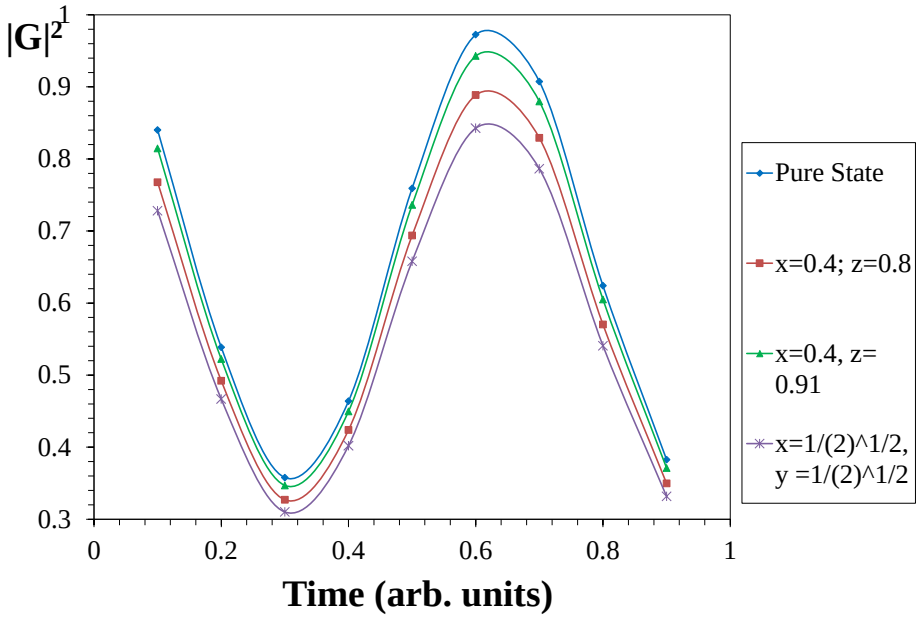

Figure 4.13. Time correlation function of the reduced dynamics of qubit 1. The system parameters are $\epsilon = -8$ meV, $\varepsilon = -2$ meV, $V = 4$ meV evaluated in the time interval $t \in [0.1, 0.9]$. The result represents the time correlation function of the closed system compared to the correlation function of the reduced dynamics of qubit 1 in the initial state $\rho = \frac{1}{2}(\mathbb{1} + a_1\sigma_x + a_3\sigma_z)$ for different values of a_1 and a_3.

Errors due to coupling with environmental spins

In Fig. (4.15) we show how the coupling to a spin bath can affect the rate of change of the evolution. As mentioned before, these results only include zz couplings. The strength of the couplings were adjusted in order to see the effects more clearly. These errors are easier to identify in the time correlation function obtained from the quantum simulation. But to better observe this effect, we looked at different regimes that are defined with respect to the parameters of the system.

Fig. (4.16), represents the evolution of a state where both qubits 1 and 2 have only z components to their density operators. The 'weak', 'intermediate' and 'strong' regimes are

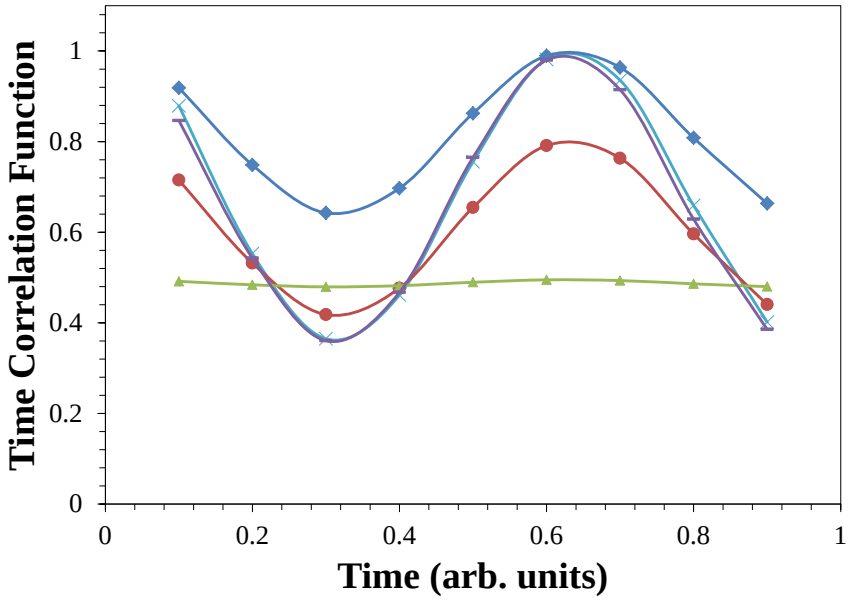

Figure 4.14. Time correlation function of the reduced dynamics of qubit 1. The system parameters are $\epsilon = -8$ meV, $\varepsilon = -2$ meV, $V = 4$ meV evaluated in the time interval $t \in [0.1, 0.9]$. The results the time correlation function of the reduced dynamics of qubit 1 for: a closed system where the two qbits are in an ideal state (case A.1 label $\times$); a system where the initial state is $\rho_1^I = \frac{1}{2}(\mathbb{1} + 0.2\sigma_x + 0.97\sigma_z)$, $\rho_1^{II} = \frac{1}{2}(\mathbb{1} + \sigma_z)$, $\rho_2^I = \rho_2^{II} = \frac{1}{2}(\mathbb{1} - \sigma_z)$ and $p = \frac{1}{2}$ (case B.2 label $-$); a system where the initial state is $\rho_1^I = \frac{1}{2}(\mathbb{1} + 0.2\sigma_x + 0.97\sigma_z)$, $\rho_1^{II} = \frac{1}{2}(\mathbb{1} - 0.2\sigma_x - 0.97\sigma_z)$, $\rho_2^I = \frac{1}{2}(\mathbb{1} - \sigma_z)$, $\rho_2^{II} = \frac{1}{2}(\mathbb{1} + \sigma_z)$ and $p = \frac{1}{2}$ (case B.2 label $\triangle$); a system where the initial state is $\rho_1^I = \frac{1}{2}(\mathbb{1} + \sigma_z)$, $\rho_1^{II} = \frac{1}{2}(\mathbb{1} - \sigma_z)$, $\rho_2^I = \frac{1}{2}(\mathbb{1} - \sigma_z)$, $\rho_2^{II} = \frac{1}{2}(\mathbb{1} + \sigma_z)$ and $p = \frac{1}{9}$ ($\bigcirc$); a system where the initial state is a maximally entangled one and qubit 2 is interacting with two additional qubits with coupling strength $J_{zz} = \frac{1}{10}$ meV ($\diamond$).

defined in terms of the strength of the coupling to the bath, J_{zz}, compared to the parameters of the system which were obtained from [56]. The coupling strength has an effect on the transfer rate. In the 'strong' regime, where the coupling strength is larger than the parameters of the system, the evolution is much slower. The 'weak' regime

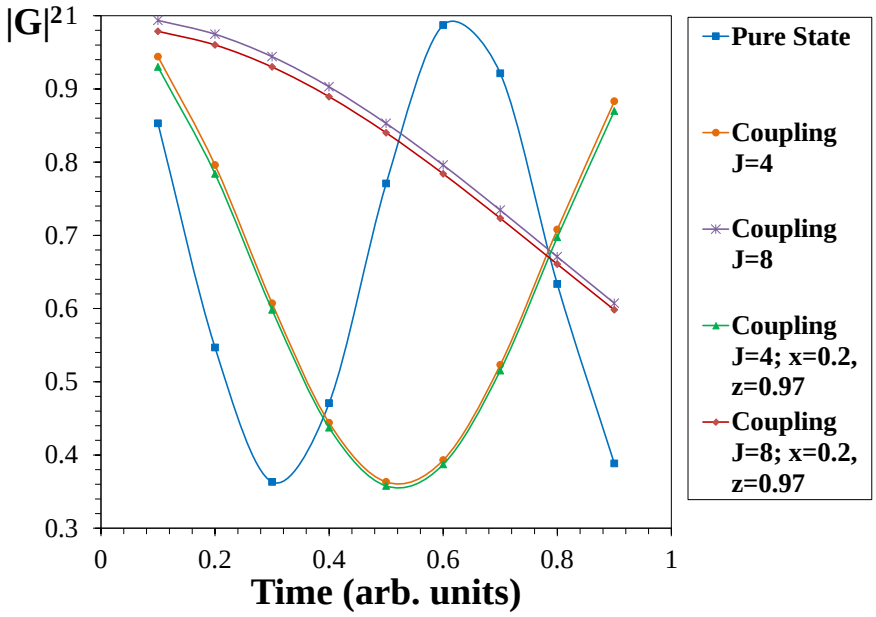

Figure 4.15. Time correlation function of the reduced dynamics of qubit 1. The system parameters are $\epsilon = -8$ meV, $\varepsilon = -2$ meV, $V = 4$ meV in the time interval $t \in [0.1, 0.9]$. The results correspond to the closed system and the system that interacts with two additional qubits, coupled only to qubit 2. The initial state of qubit 1 is $\rho = |0\rangle\langle 0|$ for one set of results, and $\rho = \frac{1}{2}(\mathbb{1} + 0.2\sigma_x + 0.97\sigma_z)$ for the other.

approximates the evolution of the system when no interaction with an external bath is present, thus making it more difficult to detect errors. These errors can be present in a quantum simulation. An AQS (recall chapter 3) is usually a simulator built using "always on" Hamiltonians, and the evolution carried out by modifying the interactions. If in the process there are interactions that are not modified properly, errors like these may arise in the final result of the simulation.

Because quantum simulations are performed on quantum systems, where access to complete information about the state at all times is not available, these errors can be detected in the final result of the simulation.

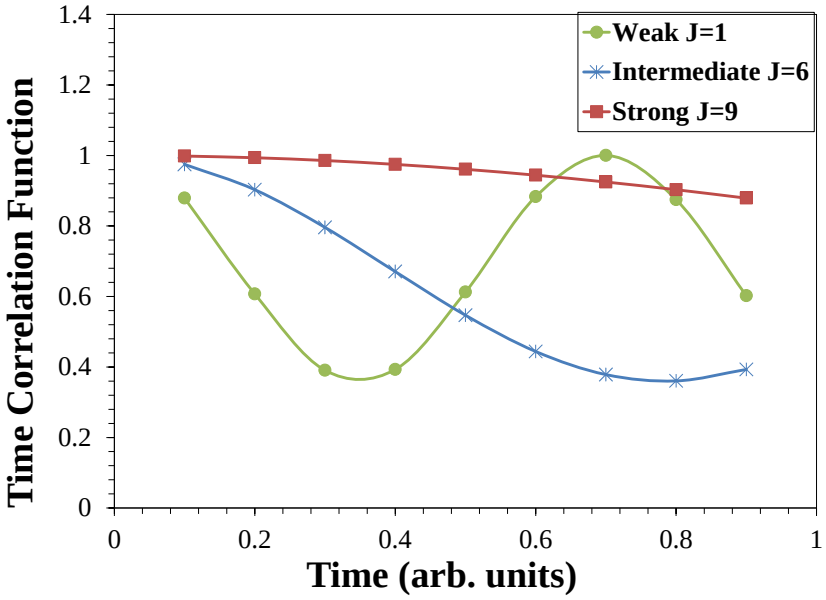

Figure 4.16. Time correlation function of the reduced dynamics of qubit 1. qubit 2 is interacting via zz coupling with qbits 3 and 4. The coupling strengths are $J_{zz} = 1$ meV in the 'weak' regime, $J_{zz} = 6$ meV in the 'intermediate' regime and $J_{zz} = 9$ meV in the 'strong' regime. The initial state of the system and bath is $|\psi\rangle = |0111\rangle$ (case A.4). The system parameters are $\epsilon = -8$ meV, $\varepsilon = -2$ meV and $V = 4$ meV, for times $t \in [0.1, 0.9]$.

.

CHAPTER 5

CONCLUSIONS

5.1 CONCLUSIONS

Interactions of quantum systems with a surrounding environment are undesirable for reliable quantum simulations and for quantum information processing in general. In order to enable the reduction or correction of noise, it is imperative that we try to understand and control or suppress the noise from the environment. Most research in error correction and fault tolerance has so far been devoted to universal quantum computing (and therefore universal quantum simulators) [109]. Lloyd's suggestion to *use* the noise to simulate the interaction of the system with the environment is clearly useful only in special cases. For some analog simulators, substantial isolation has been achieved [80]. However, other sources of noise remain in this system and in others.

It is known that interactions with the environment can lead to correlations that can result in non completely positive maps. We found that such maps are not rare in our study of a very simple model of a quantum system of fermions which can readily be simulated on a quantum computing device, or a dedicated quantum simulator. This Fano-Anderson model exhibits maps which are not completely positive for a variety of initial states, some of which were entangled and some with other non-trivial quantum correlations in the sense of non-zero quantum discord. They were shown to arise for even a fairly small transverse component to an initial density matrix which is supposed to have its Bloch vector aligned along the z axis. Thus fairly small experimental errors can lead to maps which are not completely positive in a rather simple experiment. These interactions can also cause relatively small errors in the final outcome of the measurement.

Initially correlated states, if they are not so identified, but are instead identified improperly as arising from completely positive maps, may encourage an experimenter to try to employ dynamical decoupling controls to eliminate errors. These controls will be

ineffective in these cases since local unitary transformations will not remove initial correlations or entanglement.

We have used a very specific and simple model to illustrate the effects of noise on the system including the presences of maps which are not completely positive. However, it is important to emphasize that these effects are quite general and will be present in some form in many other quantum systems including a wide class of quantum simulations.

REFERENCES

[1] R. Alicki, Phys. Rev. Lett. **75**, 3020 (1995); P. Pechukas, *ibid.*, p. 3021.

[2] A. Aspuru-Guzik and P. Walther. Photonic Quantum Simulators. *Nature*, 8:285, 2012.

[3] A. Bendersky, F. Patawski and J. P. Paz. Selective and Efficient Estimation of Parameters for Quantum Process Tomography. *Phys. Rev. Lett.*, 100:190403, 2008.

[4] A. Brodutch, A. Datta, K. Modi, A. Rivas and C. A. Rodriguez-Rosario. Vanishing quantum discord is *not* necessary for completely-positive maps. *Phys. Rev. A*, 87:042301.

[5] A. F. Fahmy, R. Marx, W. Bermel and S. J. Glaser. Thermal equilibrium as an initial state for quantum computation by NMR. *Phys. Rev. A*, 78:022317, 2008.

[6] A. M. Childs and R. Kothari. Limitations on the Simulation of non-Sparse Hamiltonians. *Qu. Inf. Comp.*, 10:669, 2010.

[7] A. M. Childs, D. Leung, L. Mancinska and M. Ozols. Characterization of Universal Two-qubit Hamiltonians. *Qu. Inf. Comp.*, 11:19, 2011.

[8] A. M. Childs, E. Farhi and J. Preskill. Robustness of adiabatic quantum computation. *Phys. Rev. A*, 65:012322, 2001. arXiv:0803.1183v2.

[9] A. Papageorgiou and C. Zhang. On the Efficiency of Quantum Algorithms for Hamiltonian Simulation. *Qu. Inf. Comp.*, 11:541, 2012.

[10] A. Pedromo-Ortiz, S. E. Venegas-Andraca and A. Aspuru-Guzik. A study of heuristic guesses for adiabatic quantum computation. *Qu. Inf. Proc.*, 10:33, 2011.

[11] A. Peres. Separability Criterion for Density Matrices. *Phys. Rev. Lett.*, 77:1413, 1996.

[12] A. R. Usha Devi and A. K .Rajagopal. Open system quantum dynamics with correlated initial states, not completely positive maps, and non-Markovianity. *Phys. Rev. A*, 83:022109, 2011.

[13] A. Rivas and S. Huelga. Open Quantum Systems. An Introduction. 2011. arXiv:1104.5242.

[14] A. Shaji and E.C.G. Sudarshan. Who's afraid of not completely positive maps? *Phys. Lett. A*, 341(1-4):48 – 54, 2005.

[15] Arvind, K. S. Mallesh and N. Mukunda. A generalized Pancharatnam geometric phase formula for three-level quantum systems. *J. Phys. A*, 30:2417–2431, 1997.

[16] B.-G. Englert and N. Metwally. Separability of entangled q-bit pairs. *J. Mod. Opt.*, 47:2221, 2000.

[17] B. M. Tehral and D. P. DiVicenzo. Problem of equilibration and the computation of correlation functions on a quantum computer. *Phys. Rev. A*, 61, 2000.

[18] B. P. Lanyon, J. D. Whitfield, G. G. Gillett, M. E. Goggin, M. P. Almeida, I. Kassal, J. D. Biamonte, M. Mohseni, B. J. Powell, M. Barbieri, A. Aspuru-Guzik and A. G. White. Towards quantum chemistry on a quantum computer. *Nature*, 2:106, 2010.

[19] Ban, M. Photon-echo technique for reducing the decoherence of a quantum bit. *J. Mod. Opt.*, 45:2315, 1998.

[20] B.M. Boghosian and W. Taylor. Simulating quantum mechanics on a quantum computer. *Physica D*, 120:30, 1998.

[21] B.P. Lanyon, C. Hempel, D. Nigg, M. Muller, R. Guerritsma, F. Zahringer, P. Schindler, J. T. Barreiro, M. Rambach, G. Kkirchmair, M. Hennrich, P. Zoller, R. Blatt and C. F. Roos. Universal Digital Quantum Simulation with Trapped Ions. *Science*, 334:57, 2011.

[22] M. S. Byrd, C. A. Bishop, and Y.-C. Ou. General open-system quantum evolution in terms of affine maps of the polarization vector. *Phys. Rev. A*, 83:012301, 2011.

[23] Byrd, M.S. and Lidar, D.A. Bang-Bang Operations from a Geometric Perspective. *Qu. Inf. Proc.*, 1:19, 2001.

[24] Byrd, M.S. and N. Khaneja. Characterization of the Positivity of the Density Matrix in Terms of the Coherence Vector Representation. *Phys. Rev. A*, 68:062322, 2003.

[25] Byrd, M.S., Wu, L.-A. and Lidar, D.A. Overview of Quantum Error Prevention and Leakage Elimination. *J. Mod. Optics*, 51:2449, 2004.

[26] C. A. Rodriguez-Rosario and E. C. G. Sudarshan. Non-Markovian Open Quantum Systems: System-Environment Correlations in Dynamical Maps. *Int. J. Quant. Inf.*, 9:1617, 2011.

[27] C. A. Rodriguez-Rosario, K. Modi, A.-M. Kuah, A. Shaji and E. C. G. Sudarshan. Completely positive maps and classical correlations. *J. Phys. A*, 41:205301, 2008.

[28] C. A. Rodriguez-Rosario, K. Modi, and A. Aspuru-Guzik. Linear assignment maps for correlated system-environment states. *Phys. Rev. A*, 81:012313, 2010.

[29] C. F. Roos, R. Gerritsma, G. Kirchmair, F. Zahringer, E. Solano and R. Blatt. Quantum Simulation of relativistic quantum physics with trapped ions. *J. Phys.: Conf. Ser*, 264:012020, 2011.

[30] C. Negrevergne, R. Somma, G. Ortiz, E. Knill, R. Laflamme. Liquid state NMR simulations of quantum many-body problems. *Phys. Rev. A*, 71:032344, 2005.

[31] C. R. Clark, T. S. Metodi, S. D. Gasster and K. R. Brown. Resource requirements for fault-tolerant quantum simulation: The ground state of the Transverse Ising Model. *Phys. Rev. A*, 79:062314, 2009.

[32] C. Zalka. Efficient Simulation of Quantum Systems by Quantum Computers, 1996. eprint quant-ph/9603026.

[33] C. Zalka. Simulating Quantum Systems on a Quantum Computer. *Proc. Roy. Soc. London Ser. A*, 454:313, 1998.

[34] Calderbank, A.R. and Shor, P.W. Good quantum error correcting codes exist. *Phys. Rev. A*, 54:1098, 1996.

[35] C.H. Bennett, J.I. Cirac, M.S. Leifer, D. W. Leung, N.Linden, S. Popescu and G. Vidal. Optimal simulation of two-qubit Hamiltonians using general local operations. *Phys. Rev. A*, 66:012305, 2002.

[36] C.H. Tseng, S. Somaroo, Y. Sharf, E. Knill, R. Laflamme, T.F. Havel, and D.G.

Cory. Quantum simulation of a three-body-interaction Hamiltonian on an NMR quantum computer. *Phys. Rev. A*, 61:012302, 2000.

[37] D. Bacon, A.M. Childs, I.L. Chuang, J. Kempe, D.W. Leung, and X. Zhou. Universal simulation of Markovian quantum dynamics, 2001.

[38] D. Deutsch. Quantum theory, the Church-Turing principle and the universal quantum computer. *Proc. Roy. Soc. London Ser. A*, 400:97, 1985.

[39] D. M. Tong, L. C. Kwek, C. H. Oh, Jing-ling Chen and L. Ma. Operator-sum representation of time-dependent density operators and its applications. *Phys. Rev. A*, 69:054102, 2004.

[40] D. Vitali and P. Tombesi. Heating and decoherence suppression using decoupling techniques. *Phys. Rev. A*, 65:012305, 2002.

[41] D. W. Berry, G. Ahokas, R. Cleve and B. C. Sanders. Efficient Quantum Algorithms for the Simulation of Sparse Hamiltonians. *Commun. Math. Phys.*, 270, 2007.

[42] D.A. Lidar and H. Wang. Calculating the Thermal Rate Constant with Exponential Speed-Up on a Quantum Computer. *Phys. Rev. E*, 59:2429–2438, 1999.

[43] D.G. Cory, R. Laflamme, E. Knill, L. Viola, T.F. Havel, N. Boulant, G. Boutis, E. Fortunato, S. Lloyd, R. Martinez, C. Negrevergne, M. Pravia, Y. Sharf, G. Teklemariam, Y.S. Weinstein, W.H. Zurek. NMR Based Quantum Information Processing: Achievements and Prospects. *Fortschritte der Physik*, 48:875, 2000.

[44] D.S. Abrams and S. Lloyd. Simulation of Many-Body Fermi Systems on a Universal Quantum Computer. *Phys. Rev. Lett.*, 79:2586, 1997.

[45] D.S. Abrams and S. Lloyd. Quantum Algorithm Providing Exponential Speed Increase for Finding Eigenvalues and Eigenvectors. *Phys. Rev. Lett.*, 83:5162–5165, 1999.

[46] L.-M Duan and G. Guo. Pulse controlled noise suppressed quantum computation. *Phys. Lett. A*, 261:139, 1999.

[47] Duan, L.-M. and Guo, G.-C. Reducing decoherence in quantum-computer memory

with all quantum bits coupling to the same environment. *Phys. Rev. A*, 57:737, 1998.

[48] E. C. G. Sudarshan, P. M. Mathews and J. Rau. Stocashtic Dynamics of Quantum-Mechanical Systems. *Phys. Rev.*, 121:920, 1961.

[49] E. Farhi, J. Goldstone, S. Gutmann and M. Sisper. Quantum Computation by Adiabatic Evolution. 2000. arXiv:quant-ph/0001106v1.

[50] E. J. Pritchett, C. Benjamin, A. Galiautdinov, M. R. Geller, A. T. Sornborger, P. C. Stancil and J. M. Martinis. Quantum Simulation of Molecular Collisions With Superconducting Qubits. 2010. arXiv:1008.0701v1.

[51] E. Jane, G. Vidal, W. Dür, P. Zoller, J.I. Cirac. Simulation of quantum dynamics with quantum optical systems. *Qu. Inf. Comp.*, 3:015, 2003.

[52] E. Knill, G. Ortiz and R. Somma. Optimal quantum measurements of expectation values of observables. *Phys. Rev. A*, 75:012328, 2007.

[53] E. R. Bittner. *Quantum Dynamics: Applications in Biological and Materials Systems*. CRC PRess, Taylor Francis Group, LLC, 2010.

[54] G. A. Alvarez and D. Suter. NMR Quantum Simulation of Localization Effects Induced by Decoherence. *Phys. Rev. Lett.*, 104:230403, 2010.

[55] G. Kimura. The Bloch Vector for N-Level Systems. *Phys. Lett. A*, 314:339, 2003.

[56] G. Ortiz, J. E. Gubernatis, E. Knill and R. Laflamme. Quantum algorithms for fermionic simulations. *Phys. Rev. A*, 64:022319, 2001.

[57] Gaitan, Frank. *Quantum Error Correction and Fault Tolerant Quantum Computing*. CRC Press, Boca Raton, FL, 2008.

[58] Gottesman, D. Class of quantum error-correcting codes saturating the quantum Hamming bound. *Phys. Rev. A*, 54:1862, 1996.

[59] Gottesman, D. *Stabilizer Codes and Quantum Error Correction*. PhD thesis, California Institute of Technology, Pasadena, CA, 1997. eprint quant-ph/9705052.

[60] G.S.Agarwal, M.O.Scully and H.Walther. Inhibition of Decoherence due to Decay in a Continuum. *Phys. Rev. Lett.*, 86:4271, 2001.

[61] H.-P. Breuer and F. Petruccione. *The theory of open quantum systems*. Oxford, Oxford, 2006.

[62] H. Wang, A. Aspuru-Guzik and M. R. Hoffmann. Quantum Algorithm for obtaining the energy spectrum of molecular systems. *Phys. Chem. Chem. Phys.*, 10:5388, 2008.

[63] H. Wang, S. Ashhab and F. Nori. Quantum algorithm for simulating the dynamics of an open quantum system. *Phys. Rev. A*, 83:062317, 2011.

[64] H. Weimer, M. Müller, I. Lesanovsky, P. Zoller and P. Büchler. A Rydberg Quantum Simulator. *Nature*, 6:328, 2010.

[65] H. Weimer, M. Müller, P. Büchler and I. Lesanovsky. Digital Quantum Simulator with Rydberg Atoms. *Qu. Inf. Comp.*, 10:885, 2011.

[66] I. Bloch, J. Dalibard and S. Nascimbene. Quantum simulations with ultra cold quantum gases. *Nature*, 8:267, 2012.

[67] I. Buluta and F. Nori. Quantum Simulators. *Science*, 326:108, 2009.

[68] I. Kassal and A. Aspuru-Guzik. Quantum algorithm for molecular properties and geometry optimization. *J. Chem. Phys.*, 131:224102, 2009.

[69] I. Kassal, J. D. Whitfield, A. Perdomo, M. H. Yung and A. Aspuru-Guzik. Simulating Chemistry Using Quantum Computers. *Annu. Rev. Phys. Chem.*, 62:185, 2011.

[70] I. Kassal, S. P. Jordan, P. J. Love, M. Mohseni and A. Aspuru-Guzik. Polynomial-time quantum algorithm for the simulation of chemical dynamics. *Proc. Nat. Acad. Sci. USA*, 105:18681, 2008.

[71] J. Cho, D. G. Angelakis and S. Bose. Simulation of high-spin Heisenberg models in coupled cavities. *Phys. Rev. A*, 78:062338, 2008.

[72] J. D. Whitfield, J. Biamonte, A. Aspuru-Guzik. Simulation of Electronic Structure Hamiltonians Using Quantum Computers. *Molecular Physics*, 109:735, 2011.

[73] J. Du, N. Xu, X. Peng, P. Wang, S. Wu and D. Lu. NMR Implementation of a Molecular Hydrogen Quantum Simulation with Adiabatic State Preparation. *Phys. Rev. Lett.*, 104:030502, 2010.

[74] J. I . Cirac and P. Zoller. Goals and opportunities in quantum simulation. *Nature*, 8:264, 2012.

[75] J. L. O'Brien, G. J. Pride, A. Gilchrist, D. F. V. James, N. K. Langford, T. C. Ralph and A. G. White. Quantum Process Tomography of a Controlled-NOT Gate. *Phys. Rev. Lett.*, 93:080502, 2004.

[76] J. Simon, W.S.Bakr, R. Ma, M. E. Tai, P. M. Preiss and M. Greiner. Quantum simulation of antiferromagnetic spin chains in an optical lattice. *Nature*, 472:307, 2011.

[77] J. Zhang, G.L. Long, W. Zhang, Z. Deng, W. Liu, Z. Lu. Simulation of heisenberg xy interactions and realization of a perfect state transfer in spin chains using liquid nuclear magnetic resonance. *Phys. Rev. A*, 72(1):012331, 2005.

[78] J.D. Biamonte, V. Bergholm, J.D. Whitfield, J. Fitzsimons and A. Aspuru-Guzik. Adiabatic Quantum Simulators. *AIP Advances*, 1:022126, 2011.

[79] Jennifer L. Dodd, Michael A. Nielsen, Michael J. Bremner, Robert T. Thew. Universal quantum computation and simulation using any entangling Hamiltonian and local unitaries. *Phys. Rev. A*, 65:040301, 2002.

[80] J.T. Barreiro, M. Muller, P. Schindler, D. Nigg, T. Monz, M. Chwalla, M. Hennrich, C. F. Roos, P. Zoller and R. Blatt. An open-system quantum simulator with trapped ions. *Nature*, 470:486, 2011.

[81] K. G. H. Vollbrecht and J. I. Cirac. Quantum simulations based on measurements and feedback control. *Phys. Rev. A*, 79:042305, 2009.

[82] K. L. Brown, S. De, V. M. Kendon and W. J. Munro. Ancilla-based quantum simulation. *New J. Phys.*, 13:095007, 2011.

[83] K. L. Brown, W. J. Munro and V. M. Kendon. Using Quantum Computers for Quantum Simulation. *Entropy*, 12:2268, 2010.

[84] K. Modi, C. A. Rodriguez-Rosario and A. Aspuru-Guzik. Positivity in the presence of initial system-environment correlations. *Phys. Rev. A*, 86:064102, 2012.

[85] K. R. Brown, C. Ospelkalus, A. C. Wilson, D. Leibfried and D. J. Wineland. Coupled quantized mechanical oscillators. *Nature*, 471:196, 2011.

[86] Kempe, J., Bacon, D., Lidar, D.A. and Whaley, K.B. Theory of Decoherence-Free, Fault-Tolerant, Universal Quantum Computation. *Phys. Rev. A*, 63:042307, 2001.

[87] Knill, E., Laflamme, R. and Viola, L. Theory of Quantum Error Correction for General Noise. *Phys. Rev. Lett.*, 84:2525–2528, 2000.

[88] K.R. Brown, R.J. Clark and I.L. Chuang. Limitations of Quantum Simulation Examined by Simulating a Pairing Hamiltonian using Nuclear Magnetic Resonance. *Phys. Rev. Lett.*, 97:050504, 2006.

[89] A.-M. Kuah, K. Modi, C. A. Rodríguez-Rosario, and E. C. G. Sudarshan. How state preparation can affect a quantum experiment: Quantum process tomography for open systems. *Phys. Rev. A*, 76:042113, 2007.

[90] L. Jakóbczyk and M. Siennicki. Geometry of Bloch vectors in two-qubit system. *Phys. Lett. A*, 286:383, 2001.

[91] Lidar, D.A. and K.B. Whaley. Decoherence-Free Subspaces and Subsystems. In *Irreversible Quantum Dynamics*. Springer-Verlag, Berlin, 2003.

[92] Lidar, D.A., Bacon, D., Kempe, J. and Whaley, K.B. Decoherence-free subspaces for multiple-qubit errors: (i) characterization. *Phys. Rev. A*, 63:022306, 2001.

[93] Lidar, D.A., Chuang, I.L. and Whaley, K.B. Decoherence free subspaces for quantum computation. *Phys. Rev. Lett.*, 81:2594, 1998.

[94] M. A. Nielsen, M. J. Bremner, J. L. Dodd, A. M. Childs, C. M. Dawson. Universal simulation of Hamiltonian dynamics for qudits. *Phys. Rev. A*, 66:022317, 2002.

[95] M. A. Pravia, Z. Chen, J. Jepez and D. G. Cory. Towards a NMR Implementation of a Quantum Lattice-Gas Algorithm. *Comp. Phys. Commun.*, 146:339, 2002.

[96] M. Asorey, A. Kossakowski, G. Marmo and E. C. G. Sudarshan. Dynamical maps and density matrices. *J. Phys. Conf. Ser*, 196:012023, 2009.

[97] M-H Yung, D. Nagaj, J. D. Whitfield and A. Aspuru-Guzik. Simulation of classical

thermal states on a quantum computer: A transfer-matrix approach. *Phys. Rev. A*, 82:060302, 2010.

[98] M. Horodecki, P. Horodecki and R. Horodecki. Separability of mixed states: necessary and sufficient conditions. *Phys. Lett. A*, 223:1, 1996.

[99] M. Johanning, A. F. Baron and C. Wunderlich. Quantum simulations with cold trapped ions. *J. of Phys. B*, 42:154009, 2009.

[100] M. McKague, M. Mosca and N. Gisin. Simulating Quantum Systems using Real Hilbert Spaces. *Phys. Rev. Lett.*, 102:020505, 2009.

[101] M. Mohseni and Lidar, D.A. Direct Characterization of Quantum Dynamics. *Phys. Rev. Lett.*, 97:170501–1–170501–4, 2006.

[102] Mahler, G. and Weberruss, V.A. *Quantum Networks: Dynamics of Open Nanostructures*. Springer Verlag, Berlin, 2nd edition, 1998.

[103] Mark S. Byrd, et al. qunet.physics.siu.edu/wiki/index.php5/Quantum_Computation_and_Quantum_Error_Prevention.

[104] N. J. Ward, I. Kassal and A. Aspuru-Guzik. Preparation of many-body states for quantum simulation. *J. Chem. Phys.*, 130:194105, 2009.

[105] N. Zuniga-Hansen, Y-C Chien and M. S. Byrd. Effects of noise, correlations and errors in the preparation of initial states in quantum simulations. *Phys. Rev. A*, 86:042335, 2012.

[106] M.A. Nielsen and I.L. Chuang. *Quantum Computation and Quantum Information*. Cambridge University Press, 2000.

[107] Harold Ollivier and Wojciech H. Zurek. Quantum discord: A measure of the quantumness of correlations. *Phys. Rev. Lett.*, 88(1):017901, 2001.

[108] P. Cappellaro, C. Ramanathan, D. G. Cory. Simulations of information transport in spin chains. *Phys. Rev. Lett.*, 99(25):250506, 2007.

[109] P. Hauke, F. M. Cucchietti, L. Tagliacozzo, I. Deutsch and M. Lewenstein. Can One

Trust Quantum Simulators? *Rep. Prog. Phys.*, 75:082401, 2012.

[110] P. Pechukas. Reduced Dynamics Need Not Be Completely Positive. *Phys. Rev. Lett.*, 73:1060, 1994.

[111] P. Wocjan, D. Janzing and T. Beth. Simulating arbitrary pair-interactions by a given Hamiltonian: Graph-Theoretical Bounds on the Time-Complexity. *Qu. Inf. Comp.*, 2:117, 2002.

[112] P. Wocjan, M. Roetteler, D. Janzing and T. Beth. Universal Simulation of Hamiltonians Using a Finite Set of Control Operations. *Qu. Inf. Comp.*, 2:133, 2001.

[113] P. Wocjan, M. Rtteler, D. Janzing, T. Beth. Simulating Hamiltonians in quantum networks: Efficient schemes and complexity bounds. *Phys. Rev. A*, 65:042309, 2001.

[114] Valentin Pavlov. Efficient quantum computing simulation. In *IEEE John Vincent Atanasoff 2006 International Symposium on Modern Computing, Proceedings*, page 235, 10662 LOS VAQUEROS CIRCLE, PO BOX 3014, LOS ALAMITOS, CA 90720-1264 USA, 2006. IEEE COMPUTER SOC. IEEE John Vincent Atanasoff International Symposium on Modern Computing, Sofia, BULGARIA, OCT 03-06, 2006.

[115] R. Alicki. Comment on "Reduced Dynamics Need Not Be Completely Positive". *Phys. Rev. Lett.*, 75:3020, 1995.

[116] R. Cleve and D. Gottesman. Efficient computations of encodings for quantum error correction. *Phys. Rev. A*, 56:76, 1997. eprint quant-ph/9607030.

[117] R. Gerritsma, B. P. Lanyon, G. Kirchmair, F. Zahringer, C. Hempel, J. Casanova, J. J. Garcia-Ripoll, E. Solano, R. Blatt and C. F. Roos. Quantum Simulation of the Klein Paradox with trapped ions. *Phys. Rev. Lett.*, 106:060503, 2011.

[118] R. Gerritsma, G. Kirchmair, F. Zahringer, E. Solano, R. Blatt and C. F. Roos. Quantum Simulation of the Dirac Equation with trapped ions. *Nature*, 463:68, 2010.

[119] R. Horodecki, P. Horodecki, M. Horodecki, K. Horodecki. Quantum entanglement. *Rev. Mod. Phys.*, 81:865, 2009.

[120] R. K. Pathria. *Statistical Mechanics*. Butterworth-Heinemann, 2001.

[121] R. Schack. Using a quantum computer to investigate quantum chaos. *Phys. Rev. A*, 57:1634, 1998. eprint quant-ph/9705016.

[122] R. Somma, G. Ortiz, E. Knill, J. Gubenartis. Quantum Simulations of Physics Problems. *Int. J. Quan. Info.*, 01:189, 2003.

[123] R. Somma, G. Ortiz, J. E. Gubernatis, E. Knill, and R. Laflamme. Simulating physical phenomena by quantum networks. *Phys. Rev. A*, 65:042323, 2002.

[124] R.P. Feynman. Simulating Physics with Computers. *Intl. J. Theor. Phys.*, 21:467, 1982.

[125] S. Bravyi, D. P. DiVincenzo, D. Loss and B. M. Terhal. Quantum Simulation of Many-Body Hamiltonians Using Perturbation Theory with Bounded-Strength Interactions. *Phys. Rev. Lett.*, 101:070503, 2008.

[126] S. Lloyd. Universal Quantum Simulators. *Science*, 273:1073, 1996.

[127] S. Mostame and R. Schtzhold1. Quantum Simulator for the Ising Model with Electrons Floating on a Helium Film. *Phys. Rev. Lett.*, 101:220501, 2008.

[128] S. Mostame, P. Rebentrost, D. I. Tsomokos and A. Aspuru-Guzik. Quantum simulator of an open quantum system using superconducting qubits: exciton transport in photosynthetic complexes. *New J. Phys.*, 2012. arXiv:1106.1683v3.

[129] S. Somaroo, C. H. Tseng, T. F. Havel, R. Laflamme, and D. G. Cory. Quantum Simulations on a Quantum Computer. *Phys. Rev. Lett.*, 82:5381, 1998.

[130] S. Wiesner. Simulations of Many-Body Quantum Systems by a Quantum Computer, 1996. eprint quant-ph/9603028.

[131] Alireza Shabani and Daniel A. Lidar. Vanishing quantum discord is necessary and sufficient for completely positive maps. *Phys. Rev. Lett.*, 102(10):100402, 2009.

[132] Shor, P.W. Scheme for reducing decoherence in quantum memory. *Phys. Rev. A*, 52:R2493, 1995.

[133] Steane, A. Quantum Computing. *Rep. Prog. Phys.*, 61:117, 1998.

[134] T.F. Jordan, A. Shaji and E. C. G. Sudarshan. Dynamics of initially entangled open quantum systems. *Phys. Rev. A*, 70:052110, 2004.

[135] V. M. Kendon, K. Nemoto and W. J. Munro. Quantum Analogue Computing. *The Royal Society A*, 368:3609, 2010.

[136] L. Viola and S. Lloyd. Dynamical suppression of decoherence in two-state quantum systems. *Phys. Rev. A*, 58:2733, 1998.

[137] Viola, L., Knill, E. and Lloyd, S. Dynamical decoupling of open quantum systems. *Phys. Rev. Lett.*, 82:2417, 1999.

[138] Viola, L., Knill, E., and Lloyd, S. Dynamical Generation of Noiseless Quantum Subsystems. *Phys. Rev. Lett.*, 85:3520, 2000.

[139] Viola, L., Lloyd, S. and Knill, E. Universal Control of Decoupled Quantum Systems. *Phys. Rev. Lett.*, 83:4888, 1999.

[140] D. Vitali and P. Tombesi. Using parity kicks for decoherence control. *Phys. Rev. A*, 59:4178, 1999.

[141] W. Dur, M. J. Bremner and H. J. Briegel. Quantum simulation of interacting high-dimensional systems: The influence of noise. *Phys. Rev. A*, 78:052325, 2008.

[142] W.H. Zurek. Decoherence and the Transition from Quantum to Classical -Revisited. *Los Alamos Science*, 27:2, 2002.

[143] W.H. Zurek. Decoherence, einselection, and the quantum origins of the classical. *Rev. Mod. Phys.*, 75:715, 2003.

[144] Wu, L.-A. and Byrd, M.S. Self-Protected Quantum Algorithms Based on Quantum State Tomography. *Qu. Inf. Proc.*, 8, 2009.

[145] Wu, L.-A., Byrd, M.S. and Lidar, D.A. Polynomial-time simulation of the BCS Hamiltonian. *Phys. Rev. Lett.*, 89:057904, 2002.

[146] X-S. Ma, B. Dakic, W. Naylor and P. Walther. Quantum Simulation of the wavefunction to probe frustrated Heisenberg spin systems. *Nature*, 7:399, 2011.

[147] Zanardi, P. Symmetrizing Evolutions. *Phys. Lett. A*, 258:77, 1999.

[148] Zanardi, P. and Rasetti, M. Noiseless Quantum Codes. *Phys. Rev. Lett.*, 79:3306, 1997.

APPENDICES

COMPOSITION OF FUNCTIONS

The composition of functions is defined as

$$(f \circ g)(x) = f(g(x))$$

Such that the function $f(x)$ becomes a function of $g(x)$. For example: given $f(x) = x^2 + x^5$ and $g(x) = 9x^3 + 2$, then:

$$(f \circ g)(x) = (9x^3 + 2)^2 + (9x^3 + 2)^5$$

Similarly, the composition of dynamical maps given by

$$B = \mathcal{T}_E \circ U_{SE} \circ \Lambda,$$

Is a function of the assignment, unitary and trace operations.

MAPPING THE FANO-ANDERSON HAMILTONIAN

This section is a repetition of the steps followed in the calculation in [56], and its intended only to demonstrate to the reader how the mapping of the original Hamiltonian was performed. The Fano-Anderson model consists of an impurity with energy ϵ surrounded by a ring of n spinless fermions, which have energies ε_{k_i}, and which interact with the impurity through the coupling strength V:

$$H = -\tau \sum_{i=1}^{n} (c_i^\dagger c_{i+1} + c_{i+1}^\dagger c_i) + \epsilon b^\dagger b + \frac{V}{\sqrt{n}} \sum_{i=1}^{n} (c_i^\dagger b + b^\dagger c_i) \tag{5.1}$$

The ring of fermions has periodic boundary conditions: $c_i^\dagger = c_{i+n}^\dagger$. The first term of the Hamiltonian in Eq. (5.1) corresponds to the ring of fermions, the c_i and $c_i^\dagger$ are the fermion creation and annihilation operators. The fermions in the ring are also allowed to jump to adjacent sites. The second term in the Hamiltonian corresponds to the the impurity site, with energy ϵ. The last term corresponds to the interaction of the impurity with the fermion sites. The discrete Fourier transform (DFT) of $c_i^\dagger$gives

$$c_{k_i}^\dagger = \frac{1}{\sqrt{n}} \sum_{j=1}^{n} e^{ik_i R_j} c_j^\dagger \tag{5.2}$$

And $R_j = ja$. Now, the inverse DFT is:

$$\sum_{k_i} c_{k_i}^\dagger e^{-ik_i R_i} = \frac{1}{\sqrt{n}} \sum_{i,j} e^{-ik_i R_i} e^{ik_i R_j} c_j^\dagger \tag{5.3}$$

where the orthogonality relation is

$$\sum_{i,j} e^{iR_j(k_i - k_j)} = n\delta_{ij} \tag{5.4}$$

So

$$c_i^\dagger = \frac{1}{\sqrt{n}} \sum_{k_i} e^{-ik_i R_i} c_{k_i}^\dagger \tag{5.5}$$

Recall that $R_i = ia$, so, if we fix the value of k_i to $k_i = k$:

$$c_i^\dagger = \frac{1}{\sqrt{n}} \sum_{i} e^{-ikia} c_k^\dagger \tag{5.6}$$

$$c_{i+1}^\dagger = \frac{1}{\sqrt{n}} \sum_{i} e^{-ikR_{i+1}} c_k^\dagger = \frac{1}{\sqrt{n}} \sum_{i}^{n} e^{-ikia} e^{-ika} c_k^\dagger \tag{5.7}$$

and,

$$c_i = \frac{1}{\sqrt{n}} \sum_{i} e^{ikia} c_k \tag{5.8}$$

$$c_{i+1} = \frac{1}{\sqrt{n}} \sum_{i}^{n} e^{ikia} e^{ika} c_k \tag{5.9}$$

So the first term in the Hamiltonian:

$$\begin{aligned} H &= -\tau \sum_{kk'} \frac{1}{n} \left[c_k^\dagger c_{k'} (e^{-ikR_i} e^{ik'Ri} e^{ik'a}) + c_k^\dagger c_{k'} (e^{-ikR_i} e^{ik'Ri} e^{-ika}) \right] \\ &= -\tau \sum_{kk'} \frac{1}{n} c_k^\dagger c_{k'} (e^{ik'a} + e^{-ika}) e^{i(k'-k)Ri} \end{aligned} \tag{5.10}$$

With,

$$\sum_{kk'} c_k^\dagger c_{k'} (e^{ik'a} + e^{-ika}) e^{i(k'-k)Ri} = n c_k^\dagger c_{k'} (e^{ik'a} + e^{-ika}) \delta_{kk'} = n c_k^\dagger c_{k'} 2\cos(ka) \tag{5.11}$$

Now define $\varepsilon_{k_i} = -2\tau\cos(k_i a)$, and for all k_i

$$\sum_{i=1}^{n} \varepsilon_{k_i} c_{k_i}^{\dagger} c_{k_i} \tag{5.12}$$

Similarly the impurity-fermion interaction part, for a fixed k

$$H_{hyb} = \frac{V}{\sqrt{n}} \sum_{i=1}^{n} \left(c_i^{\dagger} b + b^{\dagger} c_i \right) = \frac{V}{\sqrt{n}} \sum_{i=1}^{n} \left(\sum_k \frac{1}{\sqrt{n}} e^{-ikR_i} c_k^{\dagger} b + b^{\dagger} \sum_k \frac{1}{\sqrt{n}} e^{ikR_i c_k} \right) \tag{5.13}$$

Where we make use of the orthogonality relation given by Eq. (5.4), but we do it with a fixed value of $j = 0$

$$\sum_{i,j} e^{iR_i(k-0)} = n\delta_{k0} \tag{5.14}$$

Then

$$H_{hyb} = \frac{V}{\sqrt{n}} \sqrt{n} \left(c_k^{\dagger} b + b^{\dagger} c_k \right) \delta_{k,0} \tag{5.15}$$

The diagonalized wave-number representation of the Fano-Anderson Hamiltonian is given by [30, 56], where we generalize to the sum over all k_i

$$H = \sum_{i=0}^{n} \varepsilon_{k_i} c_{k_i}^{\dagger} c_{k_i} + \epsilon b^{\dagger} b + V \sum_{i=0}^{n-1} (c_{k_i}^{\dagger} b + b^{\dagger} c_{k_i}) \delta_{k_i 0}. \tag{5.16}$$

Then the following Jordan-Wigner transformations are performed:

$$b = \sigma_-^1 \tag{5.17}$$

$$b^\dagger = \sigma_+^1 \tag{5.18}$$

$$c_{k_0} = -\sigma_z^1 \sigma_-^2 \tag{5.19}$$

$$c_{k_0}^\dagger = -\sigma_z^1 \sigma_-^2 \tag{5.20}$$

$$c_{k_{n-1}} = (-1)^n \sigma_z^1 \sigma_z^2 ... \sigma_z^n \sigma_-^{n+1} \tag{5.21}$$

$$c_{k_{n-1}}^\dagger = (-1)^n \sigma_z^1 \sigma_z^2 ... \sigma_z^n \sigma_+^{n+1} \tag{5.22}$$

Where

$$\sigma_+ = \frac{\sigma_x + i\sigma_y}{2} \tag{5.23}$$

$$\sigma_- = \frac{\sigma_x - i\sigma_y}{2} \tag{5.24}$$

And by using the commutation relation $\sigma_i \sigma_j = \mathbb{1}\delta_{ij} + i\varepsilon_{ijk}\sigma_k$, the terms in the Hamiltonian become

$$b^\dagger b = \frac{1}{4}(\sigma_x + i\sigma_y)(\sigma_x + i\sigma_y) = \frac{1}{4}\left(2\mathbb{1} + i\sigma_x\sigma_y - i\sigma_y\sigma_x\right) = \frac{1}{2}\left(\mathbb{1} + \sigma_z\right) \tag{5.25}$$

$$\begin{aligned} c_{k_0}^\dagger b + b^\dagger c_{k_0} &= -\sigma_z^1 \sigma_+^2 \sigma_-^1 - \sigma_+^1 \sigma_z^1 \sigma_-^2 \\ &= -\sigma_z^1 \left(\tfrac{\sigma_x^1 + i\sigma_y^1}{2}\right)\left(\tfrac{\sigma_x^2 - i\sigma_y^2}{2}\right) - \left(\tfrac{\sigma_x^1 + i\sigma_y^1}{2}\right)\sigma_z^1\left(\tfrac{\sigma_x^2 - i\sigma_y^2}{2}\right) \\ &= \tfrac{1}{4}\left(-i\sigma_y^1\sigma_x^2 + \sigma_y^1\sigma_y^2 + \sigma_x^1\sigma_x^2 + i\sigma_x^1\sigma_y^2 + i\sigma_y^1\sigma_x^2 + \sigma_y^1\sigma_y^2 + \sigma_x^1\sigma_x^2 - i\sigma_x^1\sigma_y^2\right) \\ &= \tfrac{1}{2}\left(\sigma_x^1\sigma_x^2 + \sigma_y^1\sigma_y^2\right) \end{aligned} \tag{5.26}$$

$$c_{k_i}^{\dagger} c_{k_i} = (1)^{i+2} \left(\sigma_z^1 \sigma_z^2 ... \sigma_+^{i+2}\right) \left(\sigma_z^1 \sigma_z^2 ... \sigma_-^{i+2}\right) = \mathbb{1}_{(2^{i+1}\times 2^{i+1})} \otimes \left(\sigma_+^{i+2} \sigma_-^{i+2}\right) \tag{5.27}$$

$$= \mathbb{1}_{(2^{i+1}\times 2^{i+1})} \otimes \left(\sigma_x^{i+2} + i\sigma_y^{i+2}\right) \left(\sigma_x^{i+2} - i\sigma_y^{i+2}\right)$$

$$= \mathbb{1}_{2^{i+1}\times 2^{i+1}} \otimes \tfrac{1}{4} \left(\mathbb{1}^{i+2} - i\sigma_x^{i+2}\sigma_y^{i+2} + i\sigma_y^{i+2}\sigma_x^{i+2} + \mathbb{1}^{i+2}\right)$$

$$= \mathbb{1}_{2^{i+1}\times 2^{i+1}} \otimes \tfrac{1}{4} \left(\mathbb{1}^{i+2} + \sigma_z^{i+2} + \sigma_z^{i+2} + \mathbb{1}^{i+2}\right)$$

$$= \tfrac{1}{2} \left(\mathbb{1} + \sigma_z^{i+2}\right)$$

In this last term the subindex $(2^{i+1} \times 2^{i+1})$ in the identity operator $\mathbb{1}_{(2^{i+1}\times 2^{i+1})}$ is written to indicate its dimensionality.

Therefore we have,

$$\bar{H} = \frac{\epsilon}{2}(\mathbb{1} + \sigma_z)^1 + \frac{\varepsilon_{k_0}}{2}(\mathbb{1} + \sigma_z^2) + \frac{V}{2}(\sigma_x^1\sigma_x^2 + \sigma_y^1\sigma_y^2). \tag{5.28}$$

And the simulated Hamiltonian, by dropping the phase factor due to the identity operators, is

$$\bar{H} = \frac{\epsilon}{2}\sigma_z^1 + \frac{\varepsilon_{k_0}}{2}\sigma_z^2 + \frac{V}{2}(\sigma_x^1\sigma_x^2 + \sigma_y^1\sigma_y^2). \tag{5.29}$$

VITA

Graduate School
Southern Illinois University

Nayeli Zuniga-Hansen

nayelizh@gmail.com

Instituto Tecnologico y de Estudios Superiores de Monterrey
BSc in Physics May 2002

Dissertation Title:
OPEN QUANTUM SYSTEM DYNAMICS FOR DESCRIBING STATE TRANSFER

Major Professor: Dr. Mark S. Byrd

Publications:

- J. T. Burde, N. Zuniga-Hansen, C. L. Park and M. M. Calbi, *Kinetics of External Adsorption on Carbon Nanotube Bundles: Surface Heterogeneity Effects*, J. Phys. Chem. C, 113, 16945, 2009.
- N. Zuniga-Hansen and M. M. Calbi, *Thermal Desorption from Heterogeneous Surfaces*, J. Phys. Chem. C, 116, 5025, 2012.
- N. Zuniga-Hansen, Y-C Chien and M. S. Byrd, Effects of noise, correlations and errors in the preparation of initial states in quantum simulations, Phys. Rev. A, 86:042335, 2012.